

231072

UCRL-JC-126741
PREPRINT

Nuclear Modeling Applied to Radioisotope Production

M. G. Mustafa
M. Blann

This paper was prepared for submittal to the
International Atomic Energy Agency/Coordinated Research Project Meeting
Faure/Cape Town, South Africa
April 7-10, 1997

March 19, 1997

This is a preprint of a paper intended for publication in a journal or proceedings.
Since changes may be made before publication, this preprint is made available
with the understanding that it will not be cited or reproduced without the
permission of the author.

 Lawrence
Livermore
National
Laboratory

DISCLAIMER

This document was prepared as an account of work sponsored by an agency of the United States Government. Neither the United States Government nor the University of California nor any of their employees, makes any warranty, express or implied, or assumes any legal liability or responsibility for the accuracy, completeness, or usefulness of any information, apparatus, product, or process disclosed, or represents that its use would not infringe privately owned rights. Reference herein to any specific commercial products, process, or service by trade name, trademark, manufacturer, or otherwise, does not necessarily constitute or imply its endorsement, recommendation, or favoring by the United States Government or the University of California. The views and opinions of authors expressed herein do not necessarily state or reflect those of the United States Government or the University of California, and shall not be used for advertising or product endorsement purposes.

Nuclear Modeling Applied to Radioisotope Production

M. G. Mustafa

Lawrence Livermore National Laboratory, Livermore, CA, U. S. A. 94550

and

M. Blann, San Diego, CA, U. S. A.

Abstract

Calculated excitation functions are provided for all proton induced reactions listed for the Coordinated Research Program (CRP) on Development of a Reference Charged Particle Cross Section Data Base for Medical Radioisotope Production under the International Atomic Energy Agency (IAEA). The excitation functions are compared with experimental data sets as provided to the CRP. We discuss the merit of calculated results with respect to the experimental data.

1) Introduction

In this report we present tabular results of calculated excitation functions for production of isotopes useful as beam monitors or for medical use. This is done as part of an IAEA-CRP. The reactions considered are summarized on p2, followed by the tabular information. We present figures, some with experimental results as presented to the CRP, some with only calculated yields. These are presented following the tables.

The question to be addressed is to what degree nuclear model codes may aid in data evaluation and production. We will first give very brief comments on the comparisons between calculated excitation functions and experimental yields. We will conclude with a few subjective opinions on the question of the role of theory in evaluation. All calculated results to be presented in this work were from the HMS Alice code¹⁾, using the Monte Carlo precompound formulation, with either a Fermi gas level density, or using the shell dependent model of Kataria and Ramamurthy²⁾. The optical model was used for inverse reaction cross sections, with an energy mesh size of 0.1 MeV to 0.5 MeV in order to get smooth behavior with change of incident energy.

2) Presentation of Results

In the following we present some discussion of most of the results.

Fig. 1a, b: $^{18}\text{O}(\text{p}, \text{n})^{18}\text{F}$ - The ALICE code does not use nuclear structure information as input, nor does it contain many body break-up physics. Its use for elements as light as ^{18}O is questionable, yet it has given reasonable results in the past for targets as light as Be. We have run only the Kataria-Ramamurthy (hereafter referred to as K-R) level density option due to the double closed shell structure of ^{16}O .

Fig. 2a : $^{27}\text{Al}(\text{p}, \text{x})^{22}\text{Na}$ - The calculated result gives a good reproduction of the experimental result so far as shape goes. The peak yield is $\approx 50\%$ higher than (i.e 1.5 times) the experimental mean³⁾. The error at peak is ≈ 25 mb in a reaction cross section of ≈ 600 mb, or around 4%. Expressed in this mode, the error is not unreasonable. This point is made to emphasize that nuclear modeling codes may be expected to be best for prediction of major channels - those representing a major part of the reaction cross section, and be more speculative the smaller the fraction of the reaction cross reaction represented by the product.

Fig. 3: $^{\text{nat}}\text{Ti}(\text{p}, \text{x})^{48}\text{V}$ - The calculated result is in quite reasonable agreement with experiment, being of order 25% high at the maximum.

Fig.4a: $^{\text{nat}}\text{Ni}(\text{p}, \text{x})^{57}\text{Ni}$ - The level density model of Kataria-Ramamurthy gives a very good reproduction of the excitation function up to the peak and down to the precompound tail. The latter is somewhat underpredicted. It has long been known that shell corrected level densities are required in the Ni-Co region.

Fig. 4b: Here we show the overestimation of ^{57}Ni which results if Fermi gas level densities are used. We also show the calculated excitation function for the direct production of ^{57}Cu , which would decay into ^{57}Ni in activation measurements. Calculated ^{57}Ni excitation functions should probably add in the ^{57}Cu predicted yields, since experimental results probably represent cumulative rather than independent yields.

Fig. 6: $^{\text{nat}}\text{Cu}(\text{p}, \text{x})^{56}\text{Co}$ - The calculations give a good energy dependence for the excitation function., The Fermi gas result is nearly a factor of 2 high, the K-R result a factor of two low. The peak cross section is around 14 mb, so

the calculations are in error by 7 to 15 mb out of a reaction cross section of around 900 mb, or of order 1-2%. This again illustrates the difficulty of calculating small cross sections accurately.

Fig. 9: $^{111}\text{Cd}(\text{p},\text{n})^{111}\text{In}$ - The peak yield of around 800 mb is a major part of the reaction cross section. The calculated excitation function is in quite good agreement with the experimental results. There is some discrepancy in the threshold region, however some is likely due to error in setting the experimental energy scale since there appears to be yield below the minimum threshold Q value.

Fig. 10: $^{112}\text{Cd}(\text{p},2\text{n})^{111}\text{In}$ - Calculated and experimental yields are in excellent agreement; the peak cross section is the major fraction of the reaction cross section.

Fig. 11: $^{\text{nat}}\text{Cd}(\text{p},\text{x})^{111}\text{In}$ - The calculated yields are in excellent agreement with experimental results over the entire energy range. The data of Zaitseva appear to be based on faulty range-energy curves.

Fig. 13a: $^{127}\text{I}(\text{p},\text{x})^{123}\text{Xe}, ^{123}\text{I}$ - The calculated peak is around 35% higher than the experimental peak of around 350 mb. The calculated result also seems to 'peak' around 4 MeV below the experimental result. We show the calculated independent yields for both ^{123}Xe and ^{123}I production.

Fig. 14 a,b,c: $^{203}\text{Tl}(\text{p}, 3\text{n})^{201}\text{Pb}$ - Calculations are shown using Fermi gas and K-R level densities. Both results are in agreement with experimental results to within $\approx 10\%$, which is also the order of experimental uncertainties and spread between different data sets. Again, the peak cross sections are a major part of the reaction cross section, so we expect the modeled result to do well. The calculated shapes are not in good agreement with experimental results on the low energy side (see 14c). The experimental results seem to be somewhere in between the shapes given by the Fermi-gas and K-R level density models. The experimental results also vary significantly, and this may reflect propagation of range-energy errors in stacked foil experiments.

3. Discussions of Results/Conclusions

Nuclear model calculations are certainly useful for providing excitation functions where measurements have not, or cannot be made. They may be useful where decay scheme data necessary for activation measurements are uncertain. They should do best where the cross sections to be calculated represent a significant fraction of the total reaction cross section, and more poorly as the yields become increasingly low.

The calculations presented here for the HMS ALICE code generally gave satisfactory agreement with the experimental trends, but it is and always has been clear that good experimental data are the first choice for evaluated results. Several of the calculations presented herein agree poorly in the energy range just above threshold. It would be interesting to see if a Hauser-Feshbach calculation with nuclear structure information gave an improvement in this regime. Certainly use of the Kataria-Ramamurthy level density compensated, and indeed overcompensated for this effect for the $^{203}\text{Tl}(p, 3n)^{201}\text{Pb}$ reaction, indicating that more careful attention to details of the level density may hold a part of the answer to this question. A consideration of the accuracy of experimental cross sections is also necessary in the region; range-energy errors propagate and increase in stacked foil experiments, and may lead to large errors on a result which depends exponentially on energy.

Work performed under the auspices of the U.S. Department of Energy by the Lawrence Livermore National Laboratory under contract number W-7405-ENG-48.

References

- 1) M. Blann, Phys. Rev. C (Sept 1996)
- 2) S.K. Kataria and V.S. Ramamurthy Nuc. Phys. A349, 10 (1980)
- 3) Experimental data present in this work was provided by Dr. F. Tarkanyi, private communication Nov. 1996.

List of Tables

- | | |
|-----------|---|
| Table 1: | $^{18}\text{O}(p,n)^{18}\text{F}$ calculated excitation functions using Kataria-Ramamurthy level density tables |
| Table 2: | $^{27}\text{Al}(p,x)^{22}\text{Na}$ excitation function calculations |
| Table 3: | $^{\text{nat}}\text{Ti}(p,x)^{48}\text{V}$ excitation function calculations |
| Table 4a: | $^{\text{nat}}\text{Ni}(p,x)^{57}\text{Ni}$ excitation function calculation using K-R level density model |
| Table 4b: | $^{\text{nat}}\text{Ni}(p,x)^{57}\text{Ni}$ excitation function calculation using Fermi gas level density model |
| Table 5: | $^{\text{nat}}\text{Cu}(p,x)^{62,63,65}\text{Zn}$ excitation function calculations |
| Table 6: | $^{\text{nat}}\text{Cu}(p,x)^{56}\text{Co}$ excitation function calculations |
| Table 7: | $^{68}\text{Zn}(p,x)^{67}\text{Ga}$ excitation function calculations |
| Table 8: | $^{\text{nat}}\text{Zn}(p,x)^{67}\text{Ga}$ excitation function calculations |

- Table 9:** $^{111}\text{Cd}(\text{p},\text{n})^{111}\text{In}$ excitation function calculations
- Table 10:** $^{112}\text{Cd}(\text{p},2\text{n})^{111}\text{In}$ excitation function calculations
- Table 11:** $^{nat}\text{Cd}(\text{p},\text{x})^{111}\text{In}$ excitation function calculations
- Table 12:** $^{124}\text{Te}(\text{p},2\text{n})^{123}\text{I}$ excitation function calculations
- Table 13:** $^{127}\text{I}(\text{p},\text{x})^{123}\text{Xe}$ excitation function calculations
- Table 14:** $^{127}\text{I}(\text{p},\text{x})^{123}\text{I}$ excitation function calculations
- Table 15:** $^{203}\text{Tl}(\text{p},3\text{n})^{201}\text{Pb}$ excitation function calculations

List of Figures

- Fig. 1a) $^{18}\text{O}(\text{p},\text{n})^{18}\text{F}$ excitation function calculated with K-R level densities
- Fig. 1b) $^{18}\text{O}(\text{p},\text{n})^{18}\text{F}$ excitation function calculated with K-R level densities
- Fig. 2a) $^{27}\text{Al}(\text{p},\text{x})^{22}\text{Na}$ calculated and experimental excitation functions
- Fig. 2b) Calculated $^{27}\text{Al}(\text{p},\text{x})^{22}\text{Na}$ excitation function
- Fig. 3) $^{\text{nat}}\text{Ti}(\text{p},\text{x})^{48}\text{V}$ calculated and experimental excitation functions
- Fig. 4a) $^{\text{nat}}\text{Ni}(\text{p},\text{x})^{57}\text{Ni}$ calculated and experimental excitation functions
- Fig. 4b) $^{\text{nat}}\text{Ni}(\text{p},\text{x})^{57}\text{Ni}$, ^{57}Cu calculated (Fermi gas level densities) and experimental excitation functions
- Fig. 4c) $^{\text{nat}}\text{Ni}(\text{p},\text{x})^{57}\text{Ni}$, ^{57}Cu calculated excitation functions
- Fig. 5a) $^{\text{nat}}\text{Cu}(\text{p},\text{x})^{62,63,65}\text{Zn}$ calculated excitation functions
- Fig. 5b) $^{\text{nat}}\text{Cu}(\text{p},\text{x})^{62,63,65}\text{Zn}$ calculated excitation functions
- Fig. 6) $^{\text{nat}}\text{Cu}(\text{p},\text{x})^{56}\text{Co}$ calculated and experimental excitation function Fermi gas results x 1, dashed line; K-R x 1, solid line.
- Fig. 7a) $^{68}\text{Zn}(\text{p},\text{x})^{67}\text{Ga}$ calculated excitation function using Fermi gas level densities
- Fig. 7b) $^{68}\text{Zn}(\text{p},\text{x})^{67}\text{Ga}$ calculated excitation function using Fermi gas level densities
- Fig. 8a) $^{\text{nat}}\text{Zn}(\text{p},\text{x})^{67}\text{Ga}$ calculated excitation function using Fermi gas level densities
- Fig. 8b) $^{\text{nat}}\text{Zn}(\text{p},\text{x})^{67}\text{Ga}$ calculated excitation function using Fermi gas level densities
- Fig. 9) $^{111}\text{Cd}(\text{p},\text{n})^{111}\text{In}$ calculated and experimental excitation functions
- Fig. 10) $^{112}\text{Cd}(\text{p},\text{n})^{111}\text{In}$ calculated and experimental excitation functions
- Fig. 11a) $^{\text{nat}}\text{Cd}(\text{p},\text{x})^{111}\text{In}$ calculated and experimental excitation functions
- Fig. 11b) $^{\text{nat}}\text{Cd}(\text{p},\text{x})^{111}\text{In}$ excitation function calculated result
- Fig. 12a) $^{124}\text{Te}(\text{p},2\text{n})^{123}\text{I}$ calculated result
- Fig. 12b) $^{124}\text{Te}(\text{p},2\text{n})^{123}\text{I}$ calculated result
- Fig. 13a) $^{127}\text{I}(\text{p},\text{x})^{123}\text{Xe}$, ^{123}I calculated and experimental excitation functions.
Only primary yields shown for calculated results.
- Fig. 13b) $^{127}\text{I}(\text{p},\text{x})^{123}\text{Xe}$, ^{123}I calculated only
- Fig. 14a) $^{203}\text{Tl}(\text{p},3\text{n})^{201}\text{Pb}$ calculated and experimental excitation functions.
- Fig. 14b) $^{203}\text{Tl}(\text{p},3\text{n})^{201}\text{Pb}$ calculated and experimental excitation functions.
- Fig. 14c) $^{203}\text{Tl}(\text{p},3\text{n})^{201}\text{Pb}$ calculated and experimental excitation functions.

Table 1. $^{18}\text{O}(\text{p},\text{n})^{18}\text{F}$ excitation function calculated with level densities due to Kataria-Ramamurthy model

Elab (MeV)	Reaction Cross Section (mb)	^{18}F (mb)
2.6	448.0	0.04
2.7	466.3	0.8
2.8	488.2	2.1
2.9	505.3	4.0
3.0	521.3	6.3
3.5	585.4	23.2
4.0	628.5	52.3
4.5	651.9	90.0
5.0	665.8	118.7
5.5	677.1	150.3
6.0	690.5	173.0
6.5	708.5	197.0
7.0	726.1	214.2
7.5	742.8	238.6
8.0	751.3	249.5
9.0	743.2	261.0
10.0	713.0	236.4
11.0	679.3	195.8
12.0	654.8	163.6
13.0	635.9	135.6
14.0	624.0	113.3
16.0	615.4	81.1
18.0	618.6	61.4
20.0	615.2	48.4
25.0	557.6	29.0
30.0	505.2	19.7
35.0	477.1	15.4
40.0	451.5	12.0
50.0	407.2	8.8

Table 2: $^{27}\text{Al}(\text{p},\text{x})^{22}\text{Na}$ calculated excitation functions in mb

Elab (MeV)	Reaction Cross Section (mb)	11 25	11 24	11 23	11 22	11 21	11 20
12.0	799.7						
13.0	816.8						
14.0	821.2						
15.0	811.4			0.15			
16.0	788.0			3.5			
17.0	761.4			23.6			
18.0	737.9			43.6			
19.0	719.9			41.6			
20.0	707.9			58.1			
21.0	703.7			74.0			
23.0	702.2			90.5			
25.0	703.5			103.6			
27.0	697.3			105.1			
29.0	681.2			102.8	0.04		
31.0	659.9	0.01		88.2	2.2		
33.0	639.9	0.05		75.5	7.8		
35.0	624.3	0.22		60.7	14.1		
37.0	612.3	0.39		51.7	24.8		
39.0	601.7	0.59		44.1	36.0		
41.0	591.5	0.99	0.01	33.0	53.5		
43.0	581.1	1.28	0.08	25.8	63.4	0.02	
45.0	571.9	1.52	0.32	21.2	66.3	0.24	
50.0	547.0	1.90	2.27	16.4	59.4	1.35	
55.0	526.8	2.00	4.91	14.5	50.1	4.90	
60.0	508.3	1.78	7.74	19.9	39.1	7.75	
65.0	491.6	1.64	8.63	24.7	31.6	8.02	
70.0	476.6	1.52	8.44	32.2	26.4	6.69	0.01
80.0	450.8	1.46	7.26	38.6	25.0	5.31	0.04
90.0	428.1	1.41	6.35	35.8	28.2	4.31	0.09

Table 3: $^{nat}\text{Ti}(p,x)^{48}\text{V}$ calculated excitation functions in mb

Elab (MeV)	23 50	23 49	23 48	23 47	23 46	23 45
0.450E+01	0.186E+02	0.185E+02		0.163E+02		
0.460E+01	0.196E+02	0.195E+02		0.170E+02		
0.470E+01	0.208E+02	0.207E+02		0.185E+02		
0.480E+01	0.218E+02	0.217E+02		0.200E+02		
0.490E+01	0.228E+02	0.227E+02		0.214E+02		
0.500E+01	0.237E+02	0.237E+02	0.527E+02	0.226E+02		
0.510E+01	0.247E+02	0.246E+02	0.112E+03	0.239E+02		
0.520E+01	0.256E+02	0.256E+02	0.160E+03	0.251E+02		
0.530E+01	0.265E+02	0.265E+02	0.197E+03	0.263E+02		
0.540E+01	0.273E+02	0.274E+02	0.227E+03	0.274E+02		
0.550E+01	0.283E+02	0.282E+02	0.251E+03	0.285E+02		
0.560E+01	0.291E+02	0.291E+02	0.271E+03	0.295E+02		
0.570E+01	0.298E+02	0.299E+02	0.290E+03	0.304E+02		
0.580E+01	0.305E+02	0.307E+02	0.306E+03	0.315E+02		
0.590E+01	0.311E+02	0.314E+02	0.319E+03	0.324E+02		
0.600E+01	0.317E+02	0.320E+02	0.333E+03	0.332E+02		
0.700E+01	0.359E+02	0.366E+02	0.412E+03	0.391E+02		
0.800E+01	0.380E+02	0.388E+02	0.442E+03	0.427E+02		
0.900E+01	0.393E+02	0.399E+02	0.450E+03	0.437E+02	0.597E+01	
0.100E+02	0.404E+02	0.408E+02	0.465E+03	0.433E+02	0.117E+02	
0.110E+02	0.418E+02	0.359E+02	0.528E+03	0.375E+01	0.152E+02	
0.120E+02	0.430E+02	0.272E+02	0.485E+03	0.368E+02	0.181E+02	
0.130E+02	0.423E+02	0.220E+02	0.496E+03	0.275E+02	0.202E+02	
0.140E+02	0.352E+02	0.240E+02	0.485E+03	0.183E+02	0.221E+02	
0.150E+02	0.258E+02	0.288E+02	0.398E+03	0.125E+02	0.236E+02	
0.160E+02	0.182E+02	0.328E+02	0.310E+03	0.118E+02	0.223E+02	
0.170E+02	0.129E+02	0.347E+02	0.226E+03	0.554E+02	0.184E+02	
0.180E+02	0.938E+01	0.358E+02	0.173E+03	0.112E+03	0.133E+02	
0.190E+02	0.729E+01	0.357E+02	0.132E+03	0.159E+03	0.107E+02	
0.200E+02	0.606E+01	0.354E+02	0.100E+03	0.271E+03	0.103E+02	
0.250E+02	0.360E+01	0.309E+02	0.637E+02	0.254E+03	0.119E+02	0.306E+00
0.300E+02	0.238E+01	0.134E+02	0.458E+02	0.136E+03	0.976E+01	0.727E+00
0.350E+02	0.184E+01	0.739E+01	0.395E+02	0.681E+02	0.163E+02	0.429E+00
0.400E+02	0.152E+01	0.547E+01	0.336E+02	0.467E+02	0.298E+02	0.464E+00
0.450E+02	0.131E+01	0.443E+01	0.256E+02	0.378E+02	0.267E+02	0.342E+00
0.500E+02	0.128E+01	0.388E+01	0.210E+02	0.328E+02	0.199E+02	0.327E+00
0.550E+02	0.964E+00	0.338E+01	0.175E+02	0.288E+02	0.154E+02	0.608E+00
0.600E+02	0.867E+00	0.301E+01	0.151E+02	0.243E+02	0.113E+02	0.806E+00
0.650E+02	0.785E+00	0.261E+01	0.132E+02	0.213E+02	0.953E+01	0.689E+00
0.700E+02	0.696E+00	0.236E+01	0.118E+02	0.191E+02	0.829E+01	0.476E+00
0.750E+02	0.705E+00	0.219E+01	0.108E+02	0.179E+02	0.768E+01	0.446E+00
0.800E+02	0.581E+00	0.203E+01	0.106E+02	0.162E+02	0.728E+01	0.370E+00
0.850E+02	0.536E+00	0.190E+01	0.919E+01	0.146E+02	0.639E+01	0.368E+00
0.900E+02	0.497E+00	0.170E+01	0.844E+01	0.136E+02	0.576E+01	0.310E+00
0.950E+02	0.469E+00	0.156E+01	0.751E+01	0.127E+02	0.549E+01	0.261E+00

**Table 4a: $^{nat}\text{Ni}(p,x)^{57}\text{Ni}$ excitation functions in mb.
Kataria-Ramamurthy level density model is used.**

Elab (MeV)	28 64	28 63	28 62	28 61	28 60	28 59	28 58	28 57
0.142E+02	0.739E+00	0.370E+00	0.792E+01	0.172E+02	0.146E+03	0.154E+02	0.357E+00	
0.144E+02	0.729E+00	0.408E+00	0.770E+01	0.184E+02	0.140E+03	0.208E+02	0.333E+03	
0.146E+02	0.727E+00	0.459E+00	0.741E+01	0.195E+02	0.135E+03	0.265E+02	0.311E+03	0.158E-01
0.148E+02	0.714E+00	0.517E+00	0.712E+01	0.204E+02	0.130E+03	0.324E+02	0.300E+03	0.787E+00
0.150E+02	0.702E+00	0.571E+00	0.684E+01	0.212E+02	0.123E+03	0.386E+02	0.278E+03	0.227E+01
0.152E+02	0.692E+00	0.615E+00	0.660E+01	0.218E+02	0.120E+03	0.439E+02	0.259E+03	0.413E+01
0.154E+02	0.682E+00	0.672E+00	0.626E+01	0.224E+02	0.115E+03	0.501E+02	0.240E+03	0.652E+01
0.156E+02	0.669E+00	0.735E+00	0.605E+01	0.228E+02	0.108E+03	0.569E+02	0.224E+03	0.870E+01
0.158E+02	0.664E+00	0.780E+00	0.594E+01	0.230E+02	0.103E+03	0.628E+02	0.207E+03	0.115E+02
0.160E+02	0.660E+00	0.843E+00	0.565E+01	0.238E+02	0.970E+02	0.636E+02	0.192E+03	0.146E+02
0.162E+02	0.639E+00	0.892E+00	0.545E+01	0.240E+02	0.921E+02	0.693E+02	0.179E+03	0.173E+02
0.164E+02	0.637E+00	0.942E+00	0.517E+01	0.243E+02	0.868E+02	0.742E+02	0.167E+03	0.204E+02
0.166E+02	0.630E+00	0.100E+01	0.496E+01	0.245E+02	0.822E+02	0.801E+02	0.156E+03	0.240E+02
0.168E+02	0.631E+00	0.105E+01	0.481E+01	0.245E+02	0.777E+02	0.859E+02	0.146E+03	0.267E+02
0.170E+02	0.614E+00	0.113E+01	0.463E+01	0.247E+02	0.737E+02	0.913E+02	0.136E+03	0.301E+02
0.172E+02	0.628E+00	0.121E+01	0.452E+01	0.239E+02	0.700E+02	0.965E+02	0.128E+03	0.332E+02
0.174E+02	0.609E+00	0.127E+01	0.437E+01	0.241E+02	0.691E+02	0.106E+03	0.120E+03	0.360E+02
0.176E+02	0.613E+00	0.135E+01	0.422E+01	0.240E+02	0.659E+02	0.111E+03	0.113E+03	0.390E+02
0.178E+02	0.606E+00	0.140E+01	0.402E+01	0.241E+02	0.628E+02	0.116E+03	0.101E+03	0.443E+02
0.180E+02	0.594E+00	0.145E+01	0.394E+01	0.242E+02	0.601E+02	0.120E+03	0.948E+02	0.480E+02
0.182E+02	0.576E+00	0.151E+01	0.380E+01	0.242E+02	0.572E+02	0.125E+03	0.908E+02	0.509E+02
0.184E+02	0.574E+00	0.158E+01	0.366E+01	0.243E+02	0.520E+02	0.132E+03	0.874E+02	0.540E+02
0.186E+02	0.580E+00	0.162E+01	0.357E+01	0.242E+02	0.502E+02	0.136E+03	0.825E+02	0.581E+02
0.188E+02	0.581E+00	0.169E+01	0.349E+01	0.242E+02	0.483E+02	0.140E+03	0.801E+02	0.609E+02
0.190E+02	0.560E+00	0.175E+01	0.330E+01	0.242E+02	0.468E+02	0.144E+03	0.785E+02	0.659E+02
0.192E+02	0.575E+00	0.174E+01	0.323E+01	0.243E+02	0.455E+02	0.147E+03	0.742E+02	0.704E+02
0.194E+02	0.577E+00	0.184E+01	0.319E+01	0.243E+02	0.438E+02	0.150E+03	0.729E+02	0.741E+02
0.196E+02	0.566E+00	0.187E+01	0.312E+01	0.244E+02	0.429E+02	0.153E+03	0.699E+02	0.789E+02
0.198E+02	0.544E+00	0.195E+01	0.303E+01	0.244E+02	0.420E+02	0.156E+03	0.668E+02	0.824E+02
0.200E+02	0.581E+00	0.198E+01	0.331E+01	0.240E+02	0.406E+02	0.158E+03	0.685E+02	0.821E+02
0.250E+02	0.443E+00	0.261E+01	0.351E+01	0.222E+02	0.298E+02	0.175E+03	0.376E+02	0.177E+03
0.300E+02	0.368E+00	0.203E+01	0.448E+01	0.144E+02	0.308E+02	0.102E+03	0.305E+02	0.131E+03
0.350E+02	0.301E+00	0.156E+01	0.497E+01	0.959E+01	0.309E+02	0.644E+02	0.481E+02	0.742E+02
0.400E+02	0.263E+00	0.134E+01	0.443E+01	0.952E+01	0.271E+02	0.508E+02	0.567E+02	0.596E+02
0.450E+02	0.223E+00	0.130E+01	0.362E+01	0.950E+01	0.203E+02	0.457E+02	0.458E+02	0.529E+02
0.500E+02	0.197E+00	0.124E+01	0.311E+01	0.935E+01	0.169E+02	0.408E+02	0.365E+02	0.521E+02
0.550E+02	0.169E+00	0.115E+01	0.277E+01	0.815E+01	0.160E+02	0.372E+02	0.297E+02	0.547E+02
0.600E+02	0.162E+00	0.106E+01	0.252E+01	0.732E+01	0.147E+02	0.234E+02	0.238E+02	0.505E+02
0.650E+02	0.137E+00	0.980E+00	0.226E+01	0.657E+01	0.133E+02	0.323E+02	0.231E+02	0.445E+02
0.700E+02	0.134E+00	0.933E+00	0.218E+01	0.615E+01	0.124E+02	0.305E+02	0.219E+02	0.406E+02
0.750E+02	0.122E+00	0.926E+00	0.209E+01	0.585E+01	0.115E+02	0.288E+02	0.206E+02	0.388E+02
0.800E+02	0.107E+00	0.877E+00	0.197E+01	0.551E+01	0.107E+02	0.257E+02	0.202E+02	0.379E+02
0.850E+02	0.969E-01	0.857E+00	0.189E+01	0.534E+01	0.102E+02	0.247E+02	0.181E+02	0.390E+02
0.900E+02	0.909E-01	0.840E+00	0.178E+01	0.492E+01	0.938E+01	0.243E+02	0.163E+02	0.369E+02
0.950E+02	0.927E-01	0.798E+00	0.168E+01	0.472E+01	0.878E+01	0.238E+02	0.155E+02	0.334E+02
0.100E+03	0.802E-01	0.755E+00	0.161E+01	0.457E+01	0.865E+01	0.227E+02	0.152E+02	0.317E+02

Table 4b: $^{nat}\text{Ni}(p,x)^{57}\text{Ni}$ using Fermi gas level densities.
Calculated excitation functions are in mb.

Elab (MeV)	28 64	28 63	28 62	28 61	28 60	28 59	28 58	28 57
0.142E+02	0.760E+00	0.576E-01	0.451E+01	0.418E+01	0.730E+02	0.868E+00	0.375E+03	
0.144E+02	0.775E+00	0.777E+01	4.555E+01	0.490E+01	0.733E+02	0.270E+01	0.371E+03	
0.146E+02	0.802E+00	0.945E-01	0.464E+01	0.559E+01	0.732E+02	0.592E+01	0.366E+03	
0.148E+02	0.812E+00	0.123E+00	0.465E+01	0.623E+01	0.739E+02	0.817E+01	0.362E+03	0.109E-02
0.150E+02	0.804E+00	0.145E+00	0.468E+01	0.665E+01	0.741E+02	0.134E+02	0.359E+03	0.122E+01
0.152E+02	0.815E+00	0.177E+00	0.466E+01	0.697E+01	0.744E+02	0.196E+02	0.356E+03	0.806E+01
0.154E+02	0.816E+00	0.204E+00	0.473E+01	0.705E+01	0.748E+02	0.268E+02	0.353E+03	0.158E+02
0.156E+02	0.817E+00	0.244E+00	0.473E+01	0.704E+01	0.741E+02	0.347E+02	0.349E+03	0.257E+02
0.158E+02	0.819E+00	0.271E+00	0.473E+01	0.690E+01	0.744E+02	0.430E+02	0.346E+03	0.376E+02
0.160E+02	0.837E+00	0.305E+00	0.475E+01	0.690E+01	0.742E+02	0.513E+02	0.341E+03	0.508E+02
0.162E+02	0.823E+00	0.337E+00	0.466E+01	0.709E+01	0.741E+02	0.600E+02	0.336E+03	0.651E+02
0.164E+02	0.820E+00	0.380E+00	0.470E+01	0.728E+01	0.734E+02	0.683E+02	0.332E+03	0.802E+02
0.166E+02	0.829E+00	0.432E+00	0.465E+01	0.744E+01	0.725E+02	0.766E+02	0.326E+03	0.870E+02
0.168E+02	0.848E+00	0.475E+00	0.463E+01	0.761E+01	0.718E+02	0.846E+02	0.321E+03	0.102E+03
0.170E+02	0.842E+00	0.513E+00	0.457E+01	0.792E+01	0.711E+02	0.926E+02	0.316E+03	0.117E+03
0.172E+02	0.832E+00	0.564E+00	0.451E+01	0.814E+01	0.697E+02	0.999E+02	0.309E+03	0.133E+03
0.174E+02	0.813E+00	0.615E+00	0.455E+01	0.837E+01	0.684E+02	0.108E+03	0.303E+03	0.147E+03
0.176E+02	0.836E+00	0.672E+00	0.444E+01	0.857E+01	0.672E+02	0.115E+03	0.296E+03	0.162E+03
0.178E+02	0.827E+00	0.714E+00	0.439E+01	0.925E+01	0.660E+02	0.125E+03	0.282E+03	0.178E+03
0.180E+02	0.825E+00	0.781E+00	0.432E+01	0.943E+01	0.652E+02	0.131E+03	0.276E+03	0.186E+03
0.182E+02	0.810E+00	0.816E+00	0.431E+01	0.963E+01	0.639E+02	0.136E+03	0.267E+03	0.199E+03
0.184E+02	0.802E+00	0.882E+00	0.425E+01	0.980E+01	0.612E+02	0.143E+03	0.261E+03	0.212E+03
0.186E+02	0.828E+00	0.943E+00	0.420E+01	0.100E+02	0.606E+02	0.147E+03	0.253E+03	0.225E+03
0.188E+02	0.812E+00	0.986E+00	0.425E+01	0.102E+02	0.594E+02	0.152E+03	0.245E+03	0.237E+03
0.190E+02	0.815E+00	0.105E+01	0.407E+01	0.105E+02	0.580E+02	0.155E+03	0.239E+03	0.248E+03
0.192E+02	0.792E+00	0.109E+01	0.406E+01	0.103E+02	0.578E+02	0.156E+03	0.232E+03	0.259E+03
0.194E+02	0.813E+00	0.114E+01	0.407E+01	0.105E+02	0.568E+02	0.159E+03	0.226E+03	0.271E+03
0.196E+02	0.792E+00	0.122E+01	0.406E+01	0.107E+02	0.562E+02	0.161E+03	0.220E+03	0.280E+03
0.198E+02	0.769E+00	0.129E+01	0.398E+01	0.109E+02	0.548E+02	0.164E+03	0.213E+03	0.290E+03
0.200E+02	0.816E+00	0.132E+01	0.408E+01	0.114E+02	0.572E+02	0.165E+03	0.217E+03	0.312E+03
0.250E+02	0.593E+00	0.194E+01	0.443E+01	0.139E+02	0.409E+02	0.163E+03	0.115E+03	0.386E+03
0.300E+02	0.475E+00	0.164E+01	0.504E+01	0.975E+01	0.414E+02	0.120E+03	0.119E+03	0.205E+03
0.350E+02	0.396E+00	0.131E+01	0.538E+01	0.728E+01	0.362E+02	0.769E+02	0.154E+03	0.121E+03
0.400E+02	0.342E+00	0.122E+01	0.489E+01	0.678E+01	0.303E+02	0.562E+02	0.132E+03	0.964E+02
0.450E+02	0.296E+00	0.112E+01	0.428E+01	0.731E+01	0.255E+02	0.525E+02	0.101E+03	0.960E+02
0.500E+02	0.250E+00	0.110E+01	0.371E+01	0.722E+01	0.219E+02	0.483E+02	0.784E+02	0.925E+02
0.550E+02	0.226E+00	0.957E+00	0.331E+01	0.665E+01	0.197E+02	0.443E+02	0.680E+02	0.871E+02
0.600E+02	0.197E+00	0.906E+00	0.301E+01	0.577E+01	0.188E+02	0.403E+02	0.616E+02	0.774E+02
0.650E+02	0.184E+00	0.865E+00	0.280E+01	0.521E+01	0.168E+02	0.375E+02	0.571E+02	0.717E+02
0.700E+02	0.161E+00	0.806E+00	0.259E+01	0.485E+01	0.150E+02	0.338E+02	0.534E+02	0.691E+02
0.750E+02	0.150E+00	0.809E+00	0.249E+01	0.468E+01	0.140E+02	0.323E+02	0.499E+02	0.648E+02
0.800E+02	0.137E+00	0.800E+00	0.227E+01	0.444E+01	0.130E+02	0.305E+02	0.460E+02	0.607E+02
0.850E+02	0.133E+00	0.795E+00	0.217E+01	0.440E+01	0.127E+02	0.303E+02	0.420E+02	0.576E+02
0.900E+02	0.121E+00	0.712E+00	0.212E+01	0.415E+01	0.120E+02	0.288E+02	0.405E+02	0.554E+02
0.950E+02	0.107E+00	0.701E+00	0.200E+01	0.387E+01	0.111E+02	0.274E+02	0.390E+02	0.537E+02

Table 5: ${}^{nat}\text{Cu}(p,x){}^{62,63,65}\text{Zn}$ calculated with Fermi gas level densities. Excitation functions are in mb.

Elab (MeV)	30 65	30 64	30 63	30 62
0.220E+01				
0.230E+01	0.474E+00			
0.240E+01	0.677E+00			
0.250E+01	0.938E+00			
0.260E+01	0.126E+01			
0.270E+01	0.166E+01			
0.280E+01	0.325E+01			
0.290E+01	0.499E+01			
0.300E+01	0.628E+01			
0.310E+01	0.828E+01			
0.320E+01	0.101E+02			
0.330E+01	0.122E+02			
0.340E+01	0.146E+02			
0.350E+01	0.172E+02			
0.360E+01	0.200E+02			
0.370E+01	0.231E+02			
0.380E+01	0.263E+02			
0.390E+01	0.299E+02			
0.400E+01	0.335E+02			
0.410E+01	0.374E+02			
0.420E+01	0.413E+02			
0.430E+01	0.461E+02		0.170E+02	
0.440E+01	0.505E+02		0.349E+02	
0.450E+01	0.554E+02		0.510E+02	
0.460E+01	0.600E+02		0.651E+02	
0.470E+01	0.643E+02		0.781E+02	
0.480E+01	0.690E+02		0.896E+02	
0.490E+01	0.733E+02		0.102E+03	
0.500E+01	0.780E+02		0.113E+03	
0.510E+01	0.825E+02		0.123E+03	
0.520E+01	0.867E+02		0.133E+03	
0.530E+01	0.914E+02		0.143E+03	
0.540E+01	0.955E+02		0.152E+03	
0.550E+01	0.999E+02		0.161E+03	
0.560E+01	0.105E+03		0.169E+03	
0.570E+01	0.110E+03		0.179E+03	
0.580E+01	0.113E+03		0.187E+03	
0.590E+01	0.117E+03		0.195E+03	
0.600E+01	0.121E+03		0.202E+03	
0.610E+01	0.125E+03		0.209E+03	
0.620E+01	0.129E+03		0.216E+03	
0.630E+01	0.132E+03		0.222E+03	
0.640E+01	0.136E+03		0.228E+03	
0.650E+01	0.139E+03		0.233E+03	
0.660E+01	0.142E+03		0.238E+03	
0.680E+01	0.148E+03		0.248E+03	
0.700E+01	0.154E+03		0.257E+03	
0.720E+01	0.160E+03		0.266E+03	
0.740E+01	0.165E+03		0.275E+03	
0.760E+01	0.171E+03		0.282E+03	
0.780E+01	0.175E+03		0.289E+03	
0.800E+01	0.180E+03		0.295E+03	

Table 5 (contd.)

0.820E+01	0.185E+03	0.301E+03
0.840E+01	0.189E+03	0.309E+03
0.860E+01	0.194E+03	0.314E+03
0.880E+01	0.196E+03	0.309E+03
0.900E+01	0.200E+03	0.321E+03
0.920E+01	0.205E+03	0.326E+03
0.940E+01	0.208E+03	0.330E+03
0.960E+01	0.212E+03	0.336E+03
0.106E+02	0.223E+03	0.525E+01 0.364E+03
0.108E+02	0.216E+03	0.140E+02 0.367E+03
0.110E+02	0.207E+03	0.250E+02 0.371E+03
0.112E+02	0.189E+03	0.447E+02 0.374E+03
0.114E+02	0.177E+03	0.589E+02 0.376E+03
0.116E+02	0.163E+03	0.727E+02 0.379E+03
0.118E+02	0.150E+03	0.867E+02 0.380E+03
0.120E+02	0.138E+03	0.995E+02 0.382E+03
0.122E+02	0.127E+03	0.111E+03 0.384E+03
0.124E+02	0.122E+03	0.117E+03 0.385E+03
0.126E+02	0.112E+03	0.128E+03 0.386E+03
0.128E+02	0.102E+03	0.138E+03 0.386E+03
0.130E+02	0.935E+02	0.146E+03 0.386E+03
0.132E+02	0.857E+02	0.154E+03 0.387E+03
0.134E+02	0.787E+02	0.161E+03 0.386E+03
0.136E+02	0.718E+02	0.168E+03 0.378E+03 0.345E-01
0.138E+02	0.661E+02	0.173E+03 0.365E+03 0.731E+01
0.140E+02	0.602E+02	0.178E+03 0.348E+03 0.196E+02
0.142E+02	0.558E+02	0.183E+03 0.329E+03 0.345E+02
0.144E+02	0.546E+02	0.185E+03 0.310E+03 0.515E+02
0.146E+02	0.496E+02	0.189E+03 0.288E+03 0.709E+02
0.148E+02	0.465E+02	0.193E+03 0.268E+03 0.903E+02
0.150E+02	0.434E+02	0.196E+03 0.249E+03 0.109E+03
0.152E+02	0.403E+02	0.199E+03 0.223E+03 0.125E+03
0.154E+02	0.370E+02	0.200E+03 0.207E+03 0.131E+03
0.156E+02	0.346E+02	0.202E+03 0.192E+03 0.147E+03
0.158E+02	0.323E+02	0.206E+03 0.177E+03 0.162E+03
0.160E+02	0.308E+02	0.208E+03 0.163E+03 0.176E+03
0.162E+02	0.290E+02	0.210E+03 0.144E+03 0.195E+03
0.170E+02	0.269E+02	0.171E+03 0.984E+02 0.320E+02
0.180E+02	0.215E+02	0.174E+03 0.733E+02 0.412E+02
0.190E+02	0.185E+02	0.169E+03 0.586E+02 0.510E+02
0.200E+02	0.161E+02	0.167E+03 0.483E+02 0.599E+02
0.250E+02	0.950E+01	0.958E+02 0.258E+02 0.641E+02
0.300E+02	0.798E+01	0.406E+02 0.495E+02 0.277E+02
0.350E+02	0.673E+01	0.257E+02 0.515E+02 0.197E+02
0.400E+02	0.593E+01	0.192E+02 0.396E+02 0.180E+02
0.450E+02	0.516E+01	0.177E+02 0.290E+02 0.160E+02
0.500E+02	0.463E+01	0.153E+02 0.214E+02 0.139E+02
0.525E+02	0.415E+01	0.141E+02 0.199E+02 0.132E+02
0.550E+02	0.404E+01	0.131E+02 0.165E+02 0.116E+02
0.575E+02	0.334E+01	0.127E+02 0.172E+02 0.115E+02
0.600E+02	0.312E+01	0.109E+02 0.162E+02 0.109E+02
0.625E+02	0.303E+01	0.114E+02 0.149E+02 0.891E+01
0.650E+02	0.280E+01	0.108E+02 0.145E+02 0.963E+01
0.675E+02	0.268E+01	0.101E+02 0.133E+02 0.868E+01
0.700E+02	0.256E+01	0.980E+01 0.125E+02 0.836E+01
0.725E+02	0.254E+01	0.897E+01 0.121E+02 0.827E+01

Table 5 (contd.)

0.750E+02	0.259E+01	0.858E+01	0.119E+02	0.758E+01
0.800E+02	0.242E+01	0.840E+01	0.106E+02	0.661E+01
0.850E+02	0.214E+01	0.736E+01	0.985E+01	0.602E+01
0.900E+02	0.190E+01	0.710E+01	0.969E+01	0.611E+01
0.950E+02	0.169E+01	0.645E+01	0.852E+01	0.505E+01
0.100E+03	0.154E+01	0.596E+01	0.794E+01	0.534E+01

**Table 6: $^{nat}\text{Cu}(p,x)^{56}\text{Co}$ calculated with Fermi gas level densities.
Excitation functions are in mb.**

Elab (MeV)	27 60	27 59	27 58	27 57	27 56	27 55
0.170E+02		0.198E+00				
0.180E+02		0.620E+00				
0.190E+02		0.145E+01				
0.200E+02		0.296E+01				
0.250E+02	0.205E-05	0.107E+02	0.103E-03			
0.300E+02	0.174E+00	0.144E+02	0.319E+01			
0.350E+02	0.193E+01	0.101E+02	0.233E+02	0.407E-02		
0.400E+02	0.445E+01	0.565E+01	0.440E+02	0.211E+01		
0.450E+02	0.506E+01	0.623E+01	0.453E+02	0.251E+02		
0.480E+02	0.466E+01	0.853E+01	0.371E+02	0.445E+02	0.256E-03	
0.500E+02	0.457E+01	0.970E+01	0.300E+02	0.513E+02	0.225E-01	
0.525E+02	0.479E+01	0.119E+02	0.244E+02	0.567E+02	0.391E+00	
0.550E+02	0.469E+01	0.128E+02	0.204E+02	0.544E+02	0.263E+01	
0.575E+02	0.497E+01	0.134E+02	0.199E+02	0.512E+02	0.865E+01	0.494E-05
0.600E+02	0.454E+01	0.138E+02	0.214E+02	0.452E+02	0.149E+02	0.871E-03
0.625E+02	0.435E+01	0.138E+02	0.226E+02	0.394E+02	0.208E+02	0.177E-01
0.650E+02	0.409E+01	0.147E+02	0.243E+02	0.349E+02	0.268E+02	0.756E-01
0.675E+02	0.397E+01	0.150E+02	0.255E+02	0.320E+02	0.312E+02	0.372E+00
0.700E+02	0.376E+01	0.149E+02	0.262E+02	0.306E+02	0.322E+02	0.102E+01
0.725E+02	0.383E+01	0.153E+02	0.270E+02	0.306E+02	0.325E+02	0.195E+01
0.750E+02	0.387E+01	0.147E+02	0.272E+02	0.295E+02	0.311E+02	0.416E+01
0.800E+02	0.436E+01	0.141E+02	0.305E+02	0.298E+02	0.290E+02	0.102E+02
0.850E+02	0.459E+01	0.136E+02	0.323E+02	0.325E+02	0.226E+02	0.138E+02
0.900E+02	0.451E+01	0.131E+02	0.321E+02	0.383E+02	0.207E+02	0.144E+02
0.950E+02	0.408E+01	0.129E+02	0.307E+02	0.395E+02	0.210E+02	0.129E+02
0.100E+03	0.416E+01	0.130E+02	0.288E+02	0.397E+02	0.219E+02	0.110E+02

Kataria-Ramaurthy level densities

	27 60	27 59	27 58	27 57	27 56	27 55
0.480E+02	0.114E+02	0.103E+02	0.310E+02	0.171E+02	0.458E-05	
0.500E+02	0.132E+02	0.133E+02	0.272E+02	0.230E+02	0.956E-03	
0.525E+02	0.157E+02	0.167E+02	0.229E+02	0.282E+02	0.222E-01	
0.550E+02	0.183E+02	0.201E+02	0.198E+02	0.309E+02	0.239E+00	
0.575E+02	0.190E+02	0.224E+02	0.185E+02	0.299E+02	0.765E+00	0.214E-07
0.600E+02	0.177E+02	0.254E+02	0.196E+02	0.278E+02	0.184E+01	0.889E-05
0.625E+02	0.171E+02	0.283E+02	0.200E+02	0.258E+02	0.303E+01	0.119E-03
0.650E+02	0.158E+02	0.313E+02	0.212E+02	0.227E+02	0.452E+01	0.173E-02
0.675E+02	0.152E+02	0.325E+02	0.230E+02	0.211E+02	0.542E+01	0.153E-01
0.700E+02	0.144E+02	0.341E+02	0.246E+02	0.194E+02	0.666E+01	0.495E-01
0.725E+02	0.150E+02	0.333E+02	0.259E+02	0.187E+02	0.731E+01	0.130E+00
0.750E+02	0.161E+02	0.329E+02	0.275E+02	0.175E+02	0.739E+01	0.299E+00
0.800E+02	0.167E+02	0.312E+02	0.321E+02	0.168E+02	0.775E+01	0.838E+00
0.850E+02	0.180E+02	0.293E+02	0.347E+02	0.173E+02	0.634E+01	0.132E+01
0.900E+02	0.180E+02	0.282E+02	0.352E+02	0.197E+02	0.568E+01	0.154E+01
0.950E+02	0.164E+02	0.285E+02	0.326E+02	0.216E+02	0.532E+01	0.141E+01
0.100E+03	0.156E+02	0.282E+02	0.320E+02	0.217E+02	0.471E+01	0.132E+01

Table 7: $^{68}\text{Zn}(\text{p},\text{x})^{67}\text{Ga}$
Calculated excitation function in mb

Elab (MeV)	Reaction Cross Section (mb)	^{67}Ga (mb)
12.2	926.4	0.00
12.3	929.1	0.02
12.4	932.1	6.2
12.5	934.6	16.4
12.6	937.3	29.7
12.7	939.6	44.9
12.8	942.2	61.9
12.9	944.4	80.6
13.0	946.9	100.4
13.1	949.0	121.3
13.3	953.5	166.0
13.6	959.8	258.6
14.0	968.3	345.5
14.5	981.3	438.1
15.0	994.9	514.1
15.5	1008.4	576.5
16.0	1023.5	627.2
16.5	1039.5	668.7
17.0	1056.2	703.4
17.5	1073.4	727.3
18.0	1089.6	750.5
19.0	1119.0	773.2
21.0	1130.3	773.8
22.0	1119.1	703.9
22.5	1112.4	653.4
23.0	1107.1	601.1
23.5	1102.8	548.3
24.0	1099.1	507.3
25.0	1096.3	422.9
27.0	1109.9	282.9
30.0	1140.9	173.2
35.0	1110.3	109.6
40.0	1089.1	76.8
45.0	1067.0	64.6
50.0	1041.8	55.4
55.0	1018.7	47.9
60.0	994.2	43.4
70.0	951.9	36.9
80.0	912.9	28.3
90.0	878.9	25.1

Table 8: natZn(p,x)⁶⁷Ga calculated excitation functions in mb

Elab (MeV)	31 70	31 69	31 68	31 67	31 66
0.250E+01	0.163E-01			0.938E-01	
0.300E+01	0.107E+00			0.660E+00	
0.350E+01	0.299E+00			0.189E+01	
0.380E+01	0.459E+00		0.975E-03	0.296E+01	
0.390E+01	0.522E+00		0.147E+02	0.338E+01	
0.400E+01	0.585E+00		0.173E+02	0.381E+01	
0.420E+01	0.738E+00		0.218E+02	0.477E+01	
0.450E+01	0.983E+00		0.299E+02	0.653E+01	
0.500E+01	0.141E+01		0.432E+02	0.944E+01	
0.550E+01	0.185E+01		0.565E+02	0.124E+02	
0.600E+01	0.230E+01		0.703E+02	0.154E+02	
0.610E+01	0.239E+01		0.729E+02	0.159E+02	0.103E+02
0.620E+01	0.247E+01		0.752E+02	0.164E+02	0.226E+02
0.630E+01	0.255E+01		0.778E+02	0.170E+02	0.226E+02
0.650E+01	0.271E+01		0.823E+02	0.180E+02	0.445E+02
0.680E+01	0.293E+01		0.887E+02	0.194E+02	0.733E+02
0.700E+01	0.309E+01		0.932E+02	0.203E+02	0.849E+02
0.750E+01	0.346E+01		0.104E+03	0.225E+02	0.106E+03
0.800E+01	0.380E+01		0.113E+03	0.245E+02	0.121E+03
0.850E+01	0.413E+01		0.121E+03	0.263E+02	0.133E+03
0.900E+01	0.442E+01		0.130E+03	0.281E+02	0.143E+03
0.950E+01	0.458E+01	0.954E-01	0.137E+03	0.297E+02	0.151E+03
0.100E+02	0.425E+01	0.622E+00	0.143E+03	0.283E+02	0.158E+03
0.110E+02	0.311E+01	0.208E+01	0.151E+03	0.215E+02	0.165E+03
0.120E+02	0.211E+01	0.324E+01	0.155E+03	0.149E+02	0.170E+03
0.130E+02	0.142E+01	0.402E+01	0.138E+03	0.288E+02	0.172E+03
0.140E+02	0.993E+00	0.454E+01	0.929E+02	0.718E+02	0.170E+03
0.150E+02	0.736E+00	0.491E+01	0.624E+02	0.101E+03	0.131E+03
0.160E+02	0.600E+00	0.515E+01	0.429E+02	0.121E+03	0.942E+02
0.170E+02	0.491E+00	0.538E+01	0.307E+02	0.135E+03	0.675E+02
0.180E+02	0.430E+00	0.554E+01	0.240E+02	0.144E+03	0.555E+02
0.190E+02	0.387E+00	0.558E+01	0.195E+02	0.148E+03	0.485E+02
0.200E+02	0.347E+00	0.533E+01	0.160E+02	0.150E+03	0.448E+02
0.220E+02	0.286E+00	0.403E+01	0.119E+02	0.134E+03	0.367E+02
0.240E+02	0.260E+00	0.275E+01	0.111E+02	0.964E+02	0.296E+02
0.250E+02	0.259E+00	0.241E+01	0.104E+02	0.849E+02	0.298E+02
0.270E+02	0.239E+00	0.166E+01	0.106E+02	0.561E+02	0.340E+02
0.300E+02	0.214E+00	0.959E+00	0.110E+02	0.335E+02	0.536E+02
0.350E+02	0.174E+00	0.625E+00	0.887E+01	0.223E+02	0.648E+02
0.400E+02	0.140E+00	0.506E+00	0.646E+01	0.172E+02	0.472E+02
0.450E+02	0.127E+00	0.426E+00	0.518E+01	0.144E+02	0.293E+02
0.500E+02	0.106E+00	0.399E+00	0.432E+01	0.123E+02	0.210E+02
0.550E+02	0.928E-01	0.344E+00	0.366E+01	0.105E+02	0.169E+02
0.600E+02	0.815E-01	0.306E+00	0.341E+01	0.896E+01	0.151E+02
0.700E+02	0.678E-01	0.232E+00	0.279E+01	0.766E+01	0.115E+02
0.800E+02	0.562E-01	0.197E+00	0.215E+01	0.609E+01	0.991E+01
0.900E+02	0.497E-01	0.174E+00	0.195E+01	0.517E+01	0.812E+01

Table 9: $^{111}\text{Cd}(\text{p},\text{n})^{111}\text{In}$ calculated excitation functions in mb

Elab (MeV)	Reaction Section (mb)	Cross 111	49 110	49 109	49 108	49 107
4.2	2.3	2.3				
4.4	4.4	4.4				
4.6	6.4	6.4				
4.8	9.2	9.2				
5.0	16.3	16.3				
5.2	22.3	22.3				
5.4	32.2	32.2				
5.6	43.5	43.4				
5.8	56.1	56.0				
6.0	70.8	70.8				
6.2	87.8	87.7				
6.4	107.0	106.9				
6.6	127.9	127.9				
6.8	150.8	150.7				
7.0	177.6	177.3				
7.2	205.3	205.2				
7.4	232.6	232.0				
7.6	259.8	259.2				
7.8	287.8	287.4				
8.0	315.8	314.9				
8.2	343.6	342.7				
8.4	371.1	370.0				
8.6	401.3	399.3				
8.8	428.5	426.4				
9.0	455.2	452.7				
9.2	481.3	478.7				
9.4	506.8	503.6				
9.6	531.2	527.2				
10.0	581.3	576.0				
11.0	694.9	685.8				
12.0	797.3	679.7	0.0			
13.0	889.7	473.5	105.6			
14.0	966.4	305.2	403.9			
16.0	1073.9	147.4	787.8			
18.0	1164.9	98.4	951.9			
20.0	1245.7	79.4	1036.0	0.0		
25.0	1315.1	54.2	583.9	483.5		
30.0	1411.1	48.0	207.9	879.4	0.0	
35.0	1408.3	39.2	117.6	626.0	82.2	
40.0	1429.7	30.2	90.8	247.3	486.2	0.02
45.0	1418.4	25.9	77.2	155.2	496.1	66.7
50.0	1410.8	22.7	66.1	127.6	313.9	237.1
55.0	1391.2	20.1	59.1	114.4	186.7	294.4
60.0	1376.9	17.4	52.2	99.0	131.3	226.7
70.0	1336.1	14.5	46.1	82.5	92.2	108.9
80.0	1298.4	12.0	38.4	71.2	78.2	67.8
90.0	1261.0	11.0	30.6	59.0	65.1	55.1
100.0	1226.5	9.0	26.0	46.7	56.0	48.4

Table 10: $^{112}\text{Cd}(\text{p},2\text{n})^{111}\text{In}$ calculated excitation functions in mb

Elab (MeV)	Reaction Cross Section (mb)	49 112	49 111	49 110
11.0	700.5	692.1	0.0	
11.2	721.6	710.5	0.04	
11.4	742.9	710.5	20.5	
11.6	763.8	682.5	68.5	
11.8	784.3	642.1	27.8	
12.0	804.3	629.2	160.5	
12.2	823.3	583.0	224.5	
12.4	842.3	535.4	288.8	
12.6	860.7	490.3	350.4	
12.8	878.5	446.9	410.6	
13.0	897.3	406.4	468.7	
13.2	913.9	369.4	520.4	
13.4	929.1	332.8	570.1	
13.6	945.6	302.3	616.6	
13.8	960.1	273.6	656.8	
14.0	973.8	247.5	694.9	
14.2	986.9	226.0	729.1	
14.4	998.9	204.6	759.0	
14.6	1010.8	186.7	788.4	
14.8	1022.1	162.7	820.5	
15.0	1032.9	149.1	842.8	
15.2	1043.4	138.3	862.4	
15.4	1053.1	127.6	881.4	
15.6	1062.9	119.1	896.8	
15.8	1072.5	111.5	912.0	
16.0	1081.8	106.0	924.6	
17.2	1139.2	77.4	997.3	
17.4	1148.3	74.4	1006.0	
17.6	1157.0	73.5	1014.8	
18.0	1175.0	78.1	1023.0	
20.0	1254.3	57.7	1096.4	
20.5	1269.7	55.7	1103.8	
21.0	1280.9	51.3	1111.8	
21.5	1289.3	50.8	1100.0	0.04
22.0	1295.4	50.8	1063.5	5.6
22.5	1299.8	46.7	1003.4	31.6
23.0	1303.3	46.9	922.4	80.7
23.5	1306.5	46.0	853.4	132.7
24.0	1311.3	44.4	763.0	211.2
24.5	1317.1	43.8	673.7	298.2
25.0	1323.1	42.5	593.3	383.5
30.0	1421.0	37.8	202.5	874.0
35.0	1416.2	30.5	126.3	729.2

Table 10 (contd.)

40.0	1439.5	25.9	111.9	335.6
45.0	1428.5	23.4	93.1	188.3
50.0	1420.0	19.9	81.9	129.5
55.0	1400.5	17.0	67.9	106.3
60.0	1386.7	15.6	61.7	94.5
70.0	1345.5	12.7	50.2	77.0
80.0	1307.5	10.6	41.3	68.2
90.0	1270.0	9.6	36.0	58.8
100.0	1235.3	7.6	32.7	53.0

Table 11: $^{nat}\text{Cd}(p,x)^{111}\text{In}$ calculated excitation function in mb.

Elab (MeV)	^{111}In (mb)	Elab (MeV)	^{111}In (mb)
0.400E+01	0.000E+00	0.440E+02	0.231E+03
0.420E+01	0.295E+00	0.460E+02	0.199E+03
0.440E+01	0.561E+00	0.480E+02	0.165E+03
0.460E+01	0.827E+00	0.500E+02	0.138E+03
0.480E+01	0.119E+01	0.520E+02	0.118E+03
0.500E+01	0.210E+01	0.540E+02	0.110E+03
0.520E+01	0.287E+01	0.560E+02	0.105E+03
0.540E+01	0.414E+01	0.600E+02	0.998E+02
0.560E+01	0.559E+01	0.650E+02	0.885E+02
0.580E+01	0.721E+01	0.700E+02	0.758E+02
0.600E+01	0.911E+01	0.750E+02	0.655E+02
0.620E+01	0.113E+02	0.800E+02	0.589E+02
0.640E+01	0.138E+02	0.850E+02	0.536E+02
0.660E+01	0.164E+02	0.900E+02	0.501E+02
0.680E+01	0.194E+02	0.950E+02	0.469E+02
0.700E+01	0.228E+02	0.100E+03	0.447E+02
0.720E+01	0.264E+02		
0.740E+01	0.298E+02		
0.760E+01	0.333E+02		
0.780E+01	0.370E+02		
0.800E+01	0.405E+02		
0.820E+01	0.441E+02		
0.840E+01	0.476E+02		
0.860E+01	0.514E+02		
0.880E+01	0.548E+02		
0.900E+01	0.582E+02		
0.920E+01	0.616E+02		
0.940E+01	0.648E+02		
0.960E+01	0.678E+02		
0.100E+02	0.740E+02		
0.110E+02	0.883E+02		
0.120E+02	0.131E+03		
0.130E+02	0.176E+03		
0.140E+02	0.207E+03		
0.150E+02	0.222E+03		
0.160E+02	0.236E+03		
0.170E+02	0.248E+03		
0.180E+02	0.257E+03		
0.190E+02	0.270E+03		
0.200E+02	0.294E+03		
0.220E+02	0.325E+03		
0.240E+02	0.279E+03		
0.260E+02	0.218E+03		
0.280E+02	0.190E+03		
0.300E+02	0.190E+03		
0.320E+02	0.207E+03		
0.340E+02	0.242E+03		
0.360E+02	0.266E+03		
0.380E+02	0.279E+03		
0.400E+02	0.278E+03		
0.420E+02	0.264E+03		

Table 12: $^{124}\text{Te}(\text{p},2\text{n})^{123}\text{I}$
Calculated excitation functions in mb.

Elab (MeV)	Reaction Cross Section (mb)	53 124	53 123	53 122
11.5	714.8	704.8	0.0	
11.6	726.8	716.4	0.0	
11.7	738.7	720.8	6.7	
11.8	750.4	716.6	22.9	
11.9	761.3	703.9	45.6	
12.0	772.7	687.3	72.7	
12.0	772.7	687.9	72.7	
12.1	783.9	668.1	102.4	
12.2	794.9	645.5	134.3	
12.3	805.7	624.2	167.1	
12.4	816.3	600.7	200.4	
12.5	826.6	575.7	234.1	
12.6	836.8	552.2	268.0	
12.7	848.5	529.1	301.9	
12.8	858.3	505.1	335.3	
12.9	867.4	481.0	367.8	
13.0	876.8	458.8	399.8	
13.2	895.1	413.9	460.7	
13.4	914.0	373.0	518.7	
13.6	930.8	335.2	572.5	
13.8	947.0	301.2	619.3	
14.0	962.1	289.4	646.0	
14.2	977.0	260.9	687.4	
14.4	991.5	234.1	725.5	
14.6	1005.5	212.2	761.1	
14.8	1019.1	193.1	793.0	
15.0	1031.9	174.9	820.0	
16.0	1095.1	116.7	931.2	
17.0	1153.2	85.9	1008.6	
18.0	1202.9	70.8	1059.0	
19.0	1242.7	62.9	1096.2	
20.0	1274.5	57.4	1120.9	
21.0	1296.4	50.1	1134.6	
22.0	1314.9	50.0	1112.1	1.9
23.0	1334.4	45.7	998.1	63.0
25.0	1388.6	45.1	592.1	481.7
27.0	1443.0	42.5	346.4	790.5
30.0	1466.3	38.5	186.0	966.3
35.0	1495.8	31.2	121.8	658.6
40.0	1516.9	28.0	108.0	315.8
45.0	1516.0	22.4	97.5	173.2
50.0	1506.9	20.0	83.3	134.3
55.0	1495.9	18.4	73.8	114.3
60.0	1480.1	16.6	69.0	103.7
70.0	1443.6	13.2	55.3	88.2
80.0	1405.5	10.8	41.2	66.6
90.0	1368.7	9.4	36.0	58.3

Table 13: $^{127}\text{I}(\text{p},\text{x})^{123}\text{Xe}, ^{123}\text{I}$
Calculated excitation functions in mb.

Elab (MeV)	54 123	53 123
35.0		
36.0		
37.0		
38.0	0.001	
39.0	0.14	
40.0	1.8	0.002
41.0	9.1	0.05
42.0	32.6	0.32
43.0	68.1	1.18
44.0	115.3	3.2
45.0	171.8	6.8
46.0	248.8	12.2
47.0	305.7	19.2
48.0	359.5	29.0
49.0	376.8	39.1
50.0	415.4	51.5
51.0	471.0	66.5
53.0	472.7	92.9
55.0	435.3	111.1
57.0	376.6	131.5
60.0	292.7	152.0
63.0	215.1	156.4
65.0	177.7	153.9
70.0	124.9	144.9
75.0	101.0	135.8
80.0	92.8	131.2
85.0	81.8	126.0
90.0	75.8	112.7
95.0	66.6	112.1
100.0	63.1	109.2

Table 14: $^{127}\text{I}(\text{p},\text{x})\text{Xe,I}$
Calculated excitation functions in mb.

Elab (MeV)	Reaction Cross Section (mb)	54 127	54 126	54 125	54 124	54 123
35.0	1517.6	20.7	115.7	474.6	622.3	
36.0	1528.0	19.0	112.3	386.6	704.1	
37.0	1534.7	18.4	110.1	320.9	763.3	
38.0	1537.0	20.1	104.7	269.8	805.6	0.001
39.0	1535.8	18.1	101.3	230.7	835.2	0.14
40.0	1533.7	17.9	99.3	205.7	842.4	9.2
42.0	1531.8	16.8	91.1	163.6	829.1	32.6
43.0	1534.5	16.2	89.8	150.1	796.1	68.1
44.0	1536.0	15.7	87.4	146.4	741.1	115.3
45.0	1536.9	15.2	85.9	138.1	678.3	171.8
46.0	1536.6	15.3	79.6	128.9	602.0	248.8
47.0	1534.9	14.8	79.8	126.6	532.5	305.7
48.0	1532.1	14.7	78.2	118.6	466.0	359.5
49.0	1530.6	14.4	75.9	121.6	433.8	376.8
50.0	1527.9	14.1	72.0	117.9	382.7	415.4
51.0	1525.6	13.8	74.1	109.0	303.7	471.0
53.0	1522.5	13.3	72.9	104.4	245.9	472.7
55.0	1519.8	13.3	69.4	99.6	222.2	435.3
57.0	1514.8	12.2	68.2	95.2	196.4	376.6
60.0	1501.5	10.8	63.8	87.9	180.2	292.7
63.0	1490.7	10.9	59.9	81.5	152.9	177.7
70.0	1468.6	10.5	52.1	80.4	136.3	124.9
75.0	1447.5	8.3	49.0	71.0	122.5	101.0
80.0	1429.3	8.2	44.6	66.0	111.1	92.8
85.0	1410.2	7.3	41.0	61.5	106.0	81.8
90.0	1392.4	7.3	37.9	58.4	94.7	75.8
95.0	1374.8	6.6	36.3	53.9	88.0	66.6
100.0	1356.8	6.2	34.4	50.4	81.7	63.1
Elab (MeV)	Reaction Cross Section (mb)	53 127	53 126	53 125	53 124	53 123
35.0	1517.6	37.8	97.0	129.2	3.0	
36.0	1528.0	37.6	100.2	141.8	7.1	
37.0	1534.7	34.9	99.8	152.8	14.4	
38.0	1537.0	35.7	99.3	157.6	23.5	
39.0	1535.8	34.1	97.3	162.5	34.5	
40.0	1533.7	32.7	97.6	165.3	47.2	0.002
41.0	1532.1	32.3	97.8	164.5	64.8	0.05
42.0	1531.8	32.8	96.7	162.7	78.8	0.3
43.0	1534.5	31.2	96.3	162.9	93.6	1.2
44.0	1536.0	31.5	95.7	162.1	106.7	3.2
45.0	1536.9	30.2	95.4	164.1	117.9	6.7
46.0	1536.6	30.2	94.4	163.7	126.4	12.2
47.0	1534.9	30.4	93.7	165.4	130.3	19.2
48.0	1532.1	29.8	94.3	165.7	136.7	29.0
49.0	1530.6	27.7	94.1	164.1	141.7	39.1
50.0	1527.9	28.4	94.3	163.6	142.3	51.5

Table 14 (contd.)

Elab (MeV)	Reaction Cross Section (mb)	53 127	53 126	53 125	53 124	53 123	53 122
51.0	1525.6	29.6	97.4	160.5	141.0	66.5	0.02
53.0	1522.5	28.8	95.2	157.3	139.1	92.9	0.34
55.0	1519.8	26.3	94.8	158.0	144.9	111.1	0.9
57.0	1514.8	24.8	92.0	155.9	143.7	131.5	4.2
60.0	1501.5	23.9	92.8	153.3	140.8	152.0	17.7
63.0	1490.7	23.1	90.7	159.1	139.2	156.4	32.9
65.0	1484.4	22.9	86.1	155.6	138.2	153.9	54.2
70.0	1468.6	20.9	85.8	150.0	134.0	144.9	96.3
75.0	1447.5	19.9	82.5	148.1	132.5	135.8	112.0
80.0	1429.3	17.9	83.4	144.5	132.0	131.2	111.9
85.0	1410.2	16.2	82.0	143.0	127.6	126.0	100.7
90.0	1392.4	16.8	78.5	136.8	117.0	112.1	88.6
100.0	1356.8	14.0	75.6	133.2	115.5	109.2	85.2

Table 15: $^{203}\text{Tl}(\text{p},3\text{n})^{201}\text{Pb}$
Calculated excitation functions in mb.

Elab (mev)	Reaction Cross Section (mb)	82 203	82 202	82 201
17.8	1078.9	33.5	1031.8	0.5
17.9	1088.1	33.7	1037.4	1.6
18.0	1097.7	33.5	1045.5	3.6
18.1	1106.7	34.3	1047.6	6.8
18.2	1117.1	33.1	1054.2	11.7
18.3	1126.0	33.7	1053.2	18.4
18.4	1134.8	33.5	1053.6	27.0
18.5	1143.5	33.7	1047.8	37.9
18.6	1152.1	33.4	1042.3	50.9
18.7	1161.9	34.7	1033.3	65.8
18.8	1170.4	33.7	1025.1	83.2
18.9	1179.3	33.7	1011.9	102.1
19.1	1195.8	33.9	981.5	145.8
19.3	1211.9	33.2	944.7	196.0
19.5	1227.6	33.9	928.4	224.0
19.7	1242.9	33.4	885.8	280.7
19.9	1258.3	32.4	839.4	341.3
20.1	1272.7	32.8	792.0	401.3
20.3	1286.8	32.5	743.4	462.5
20.5	1300.4	33.4	694.0	522.9
20.7	1313.6	31.9	648.2	581.6
20.9	1326.8	33.5	601.4	638.9
21.0	1333.0	32.6	582.8	665.1
22.0	1394.0	30.8	402.7	905.6
23.0	1445.9	29.6	290.3	1070.5
24.0	1494.3	28.7	226.5	1181.0
25.0	1543.4	28.7	182.6	1269.8
26.0	1587.2	28.0	159.5	1319.7
27.0	1624.8	27.5	145.7	1287.3
28.0	1654.8	27.4	134.5	1150.5
29.0	1681.9	25.9	125.2	975.7
30.0	1704.6	24.1	120.5	744.3
31.0	1727.6	22.8	114.3	570.7
32.0	1753.9	23.0	108.7	437.0
33.0	1789.1	21.8	104.7	344.5
34.0	1807.9	21.5	102.3	282.2
35.0	1828.9	20.3	100.0	248.7
40.0	1883.0	20.3	92.0	170.8
45.0	1937.9	18.4	79.1	139.7
50.0	1964.0	13.9	68.0	118.6
55.0	1974.7	13.4	62.3	104.1
60.0	1985.6	11.8	55.6	93.4
65.0	1979.8	10.8	51.6	87.6
70.0	1975.6	10.4	46.4	79.2
75.5	1965.4	8.7	43.0	73.9
80.0	1952.5	7.9	40.1	69.1
85.0	1940.4	8.2	39.8	64.5
90.0	1924.7	7.0	36.0	58.8
95.0	1909.6	6.5	33.6	57.7

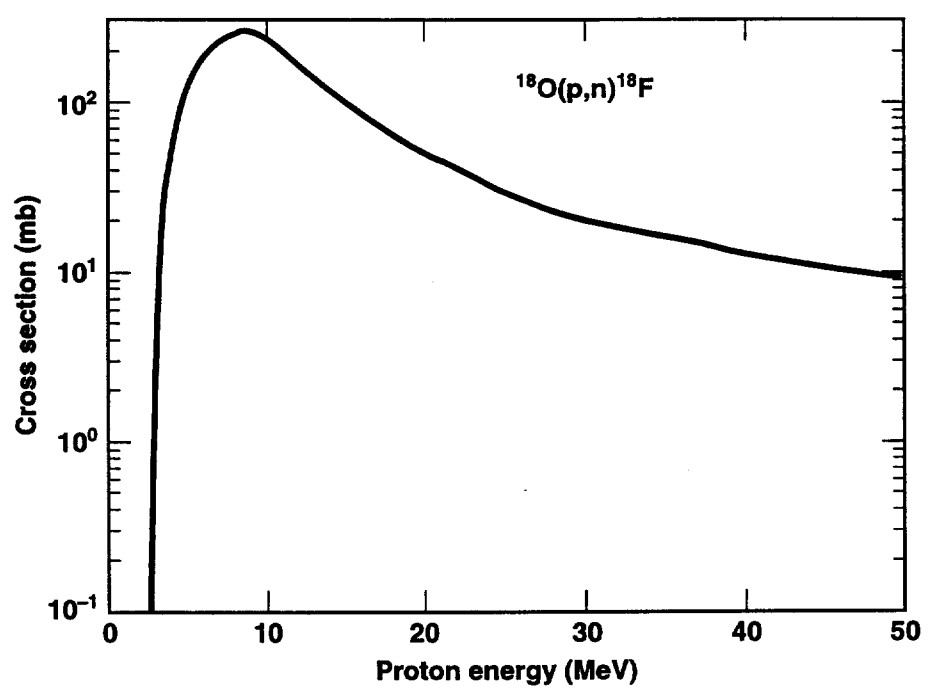


Figure 1a.

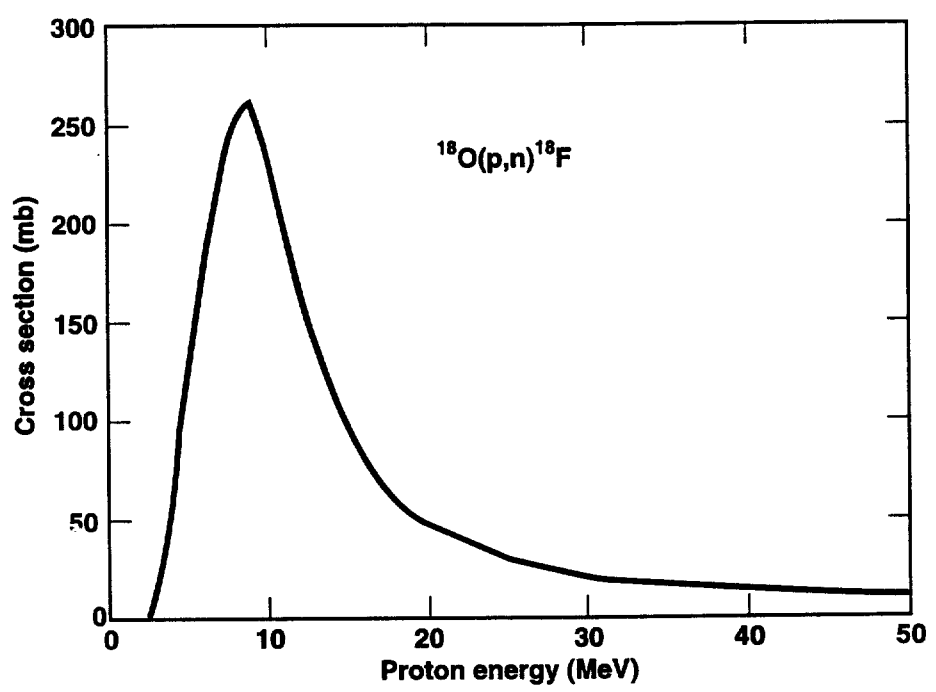


Figure 1b.

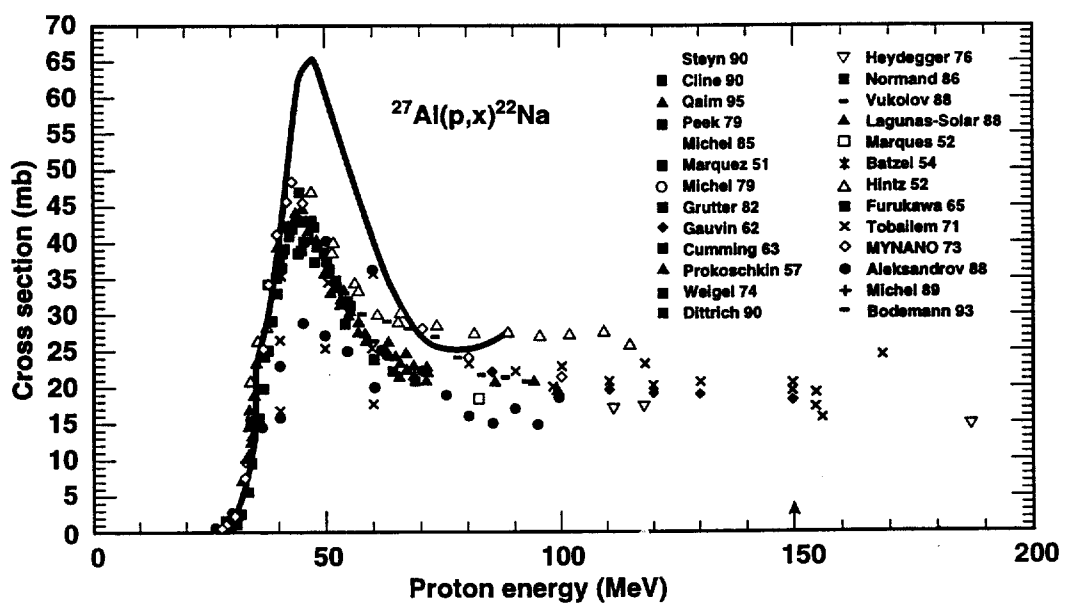


Figure 2a.

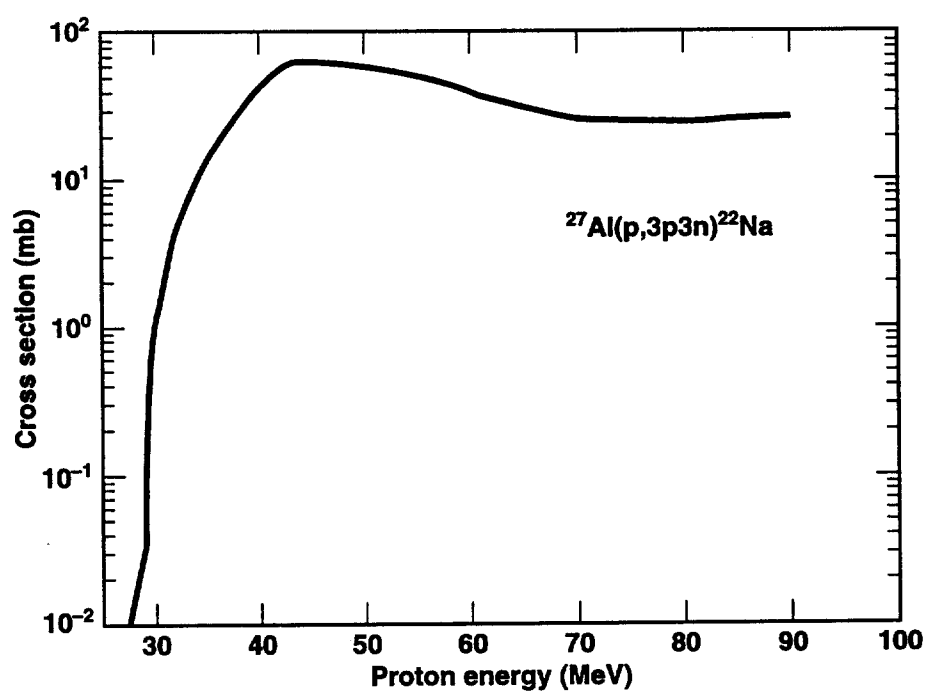


Figure 2b.

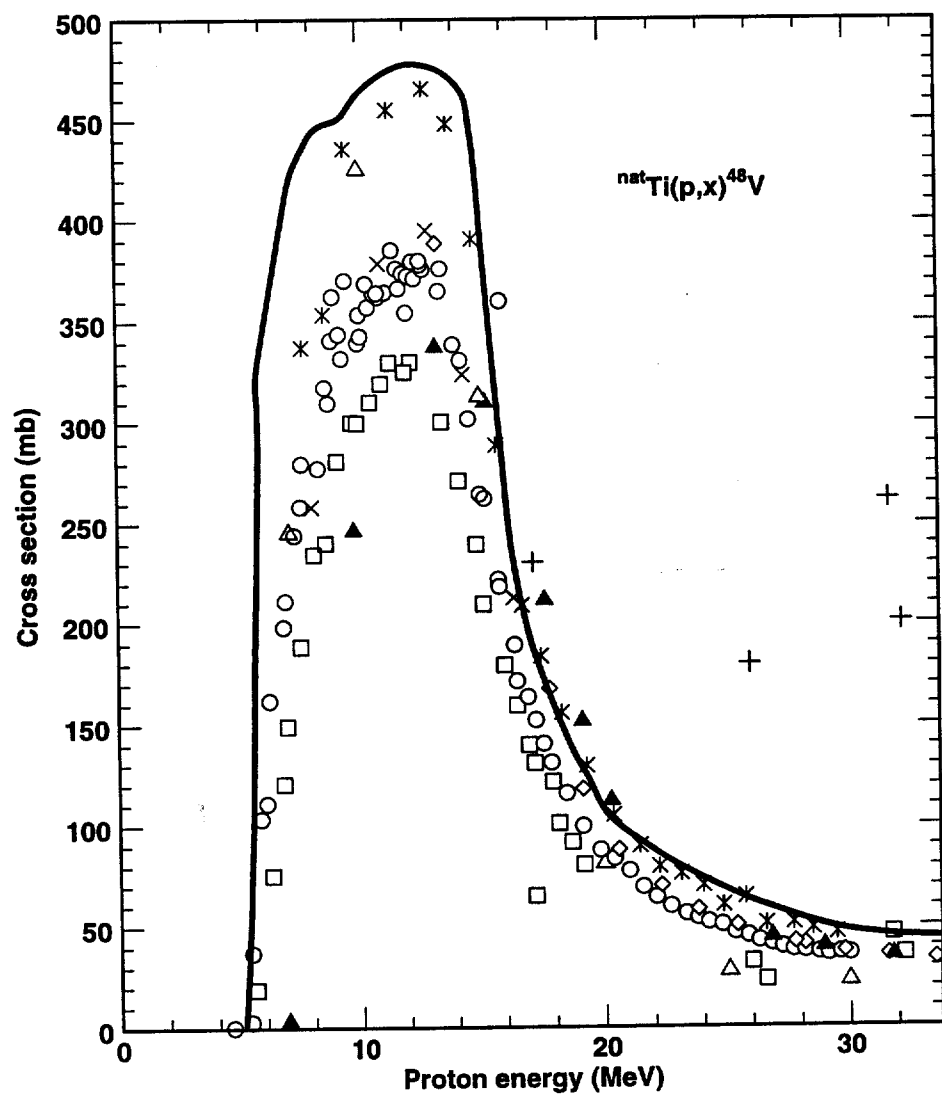


Figure 3.

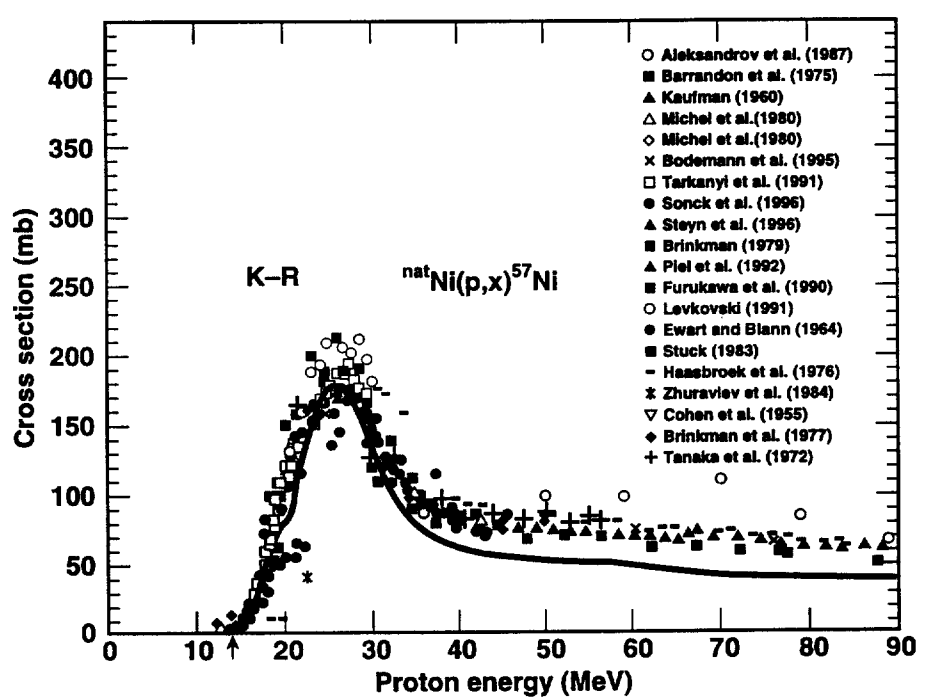


Figure 4a.

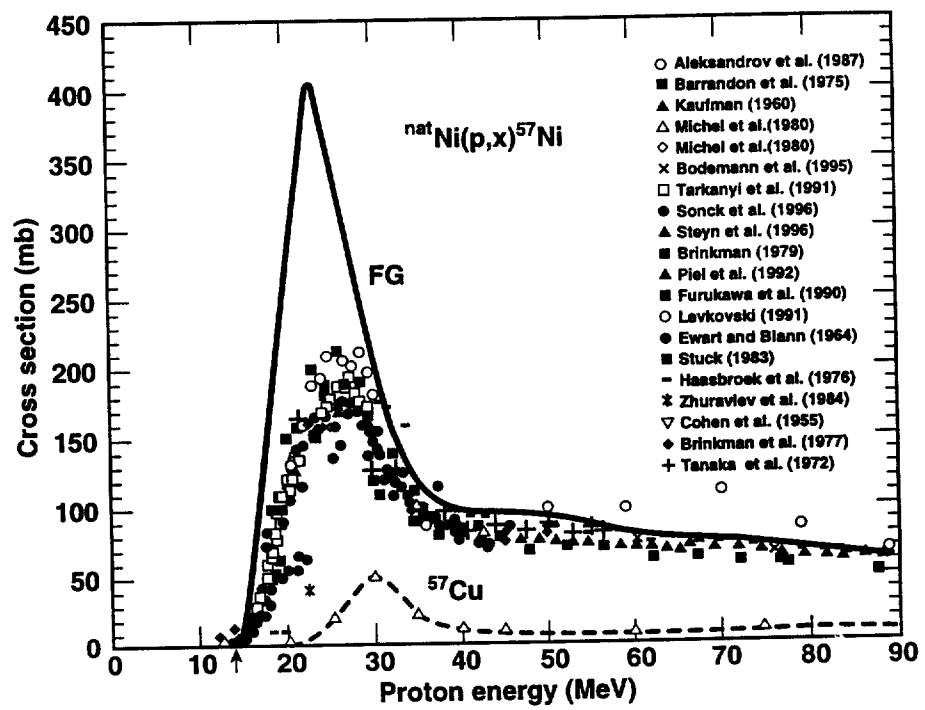


Figure 4b.

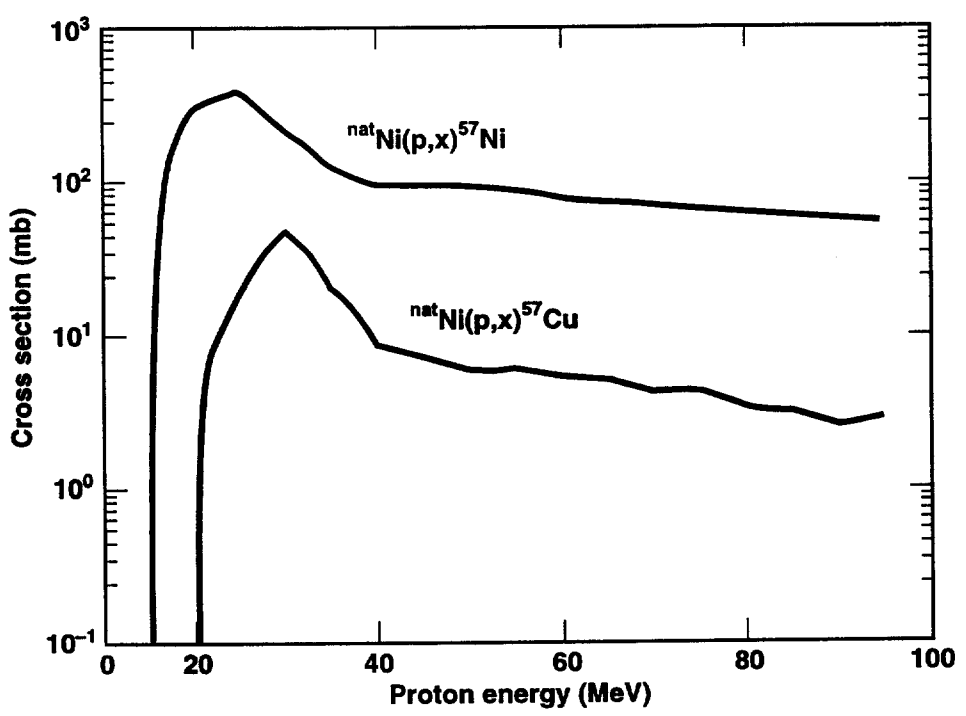


Figure 4c.

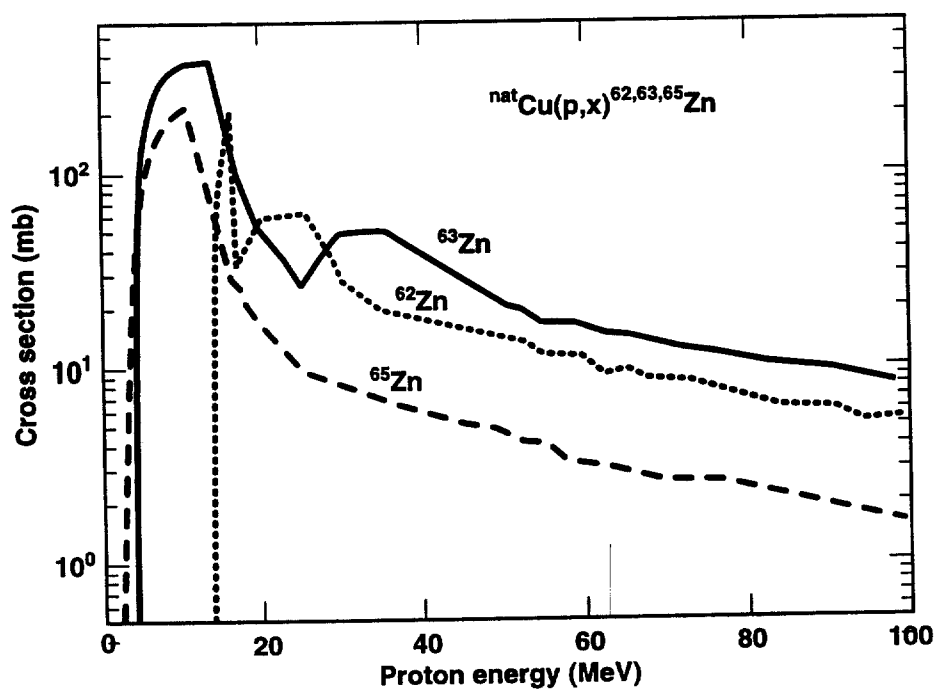


Figure 5a.

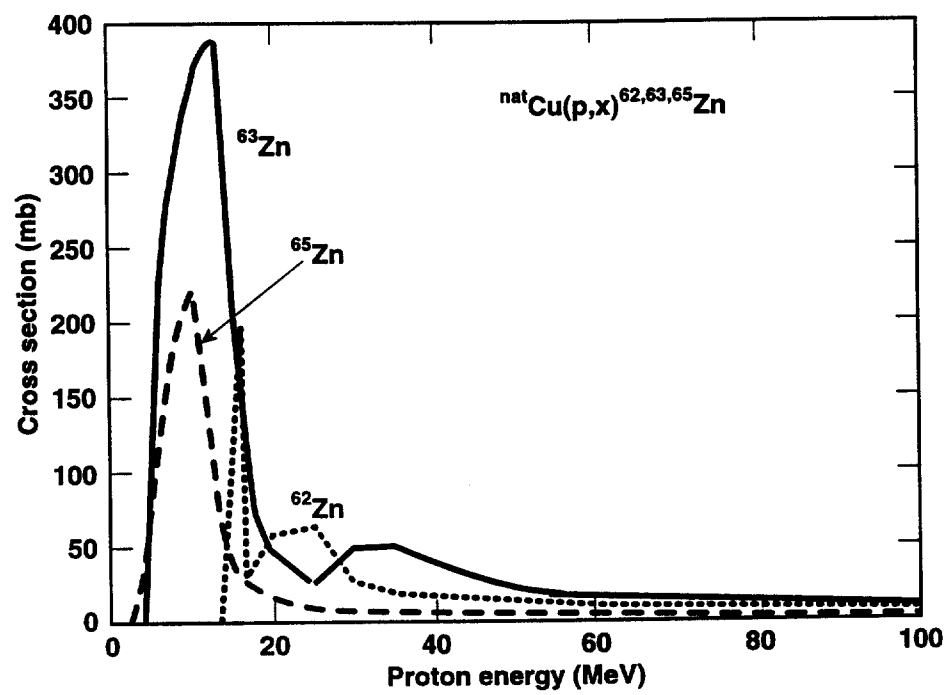


Figure 5b.

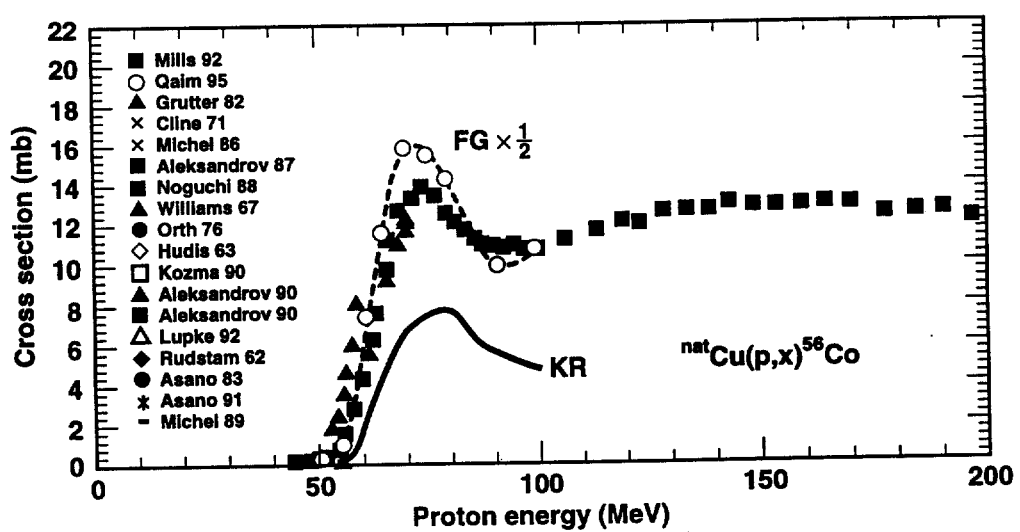


Figure 6.

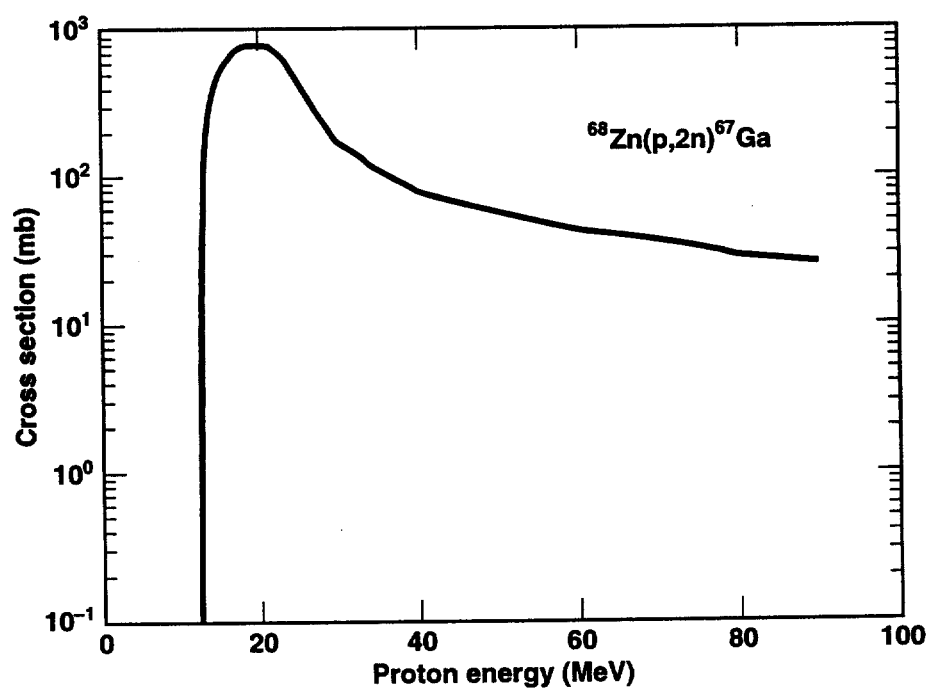


Figure 7a.

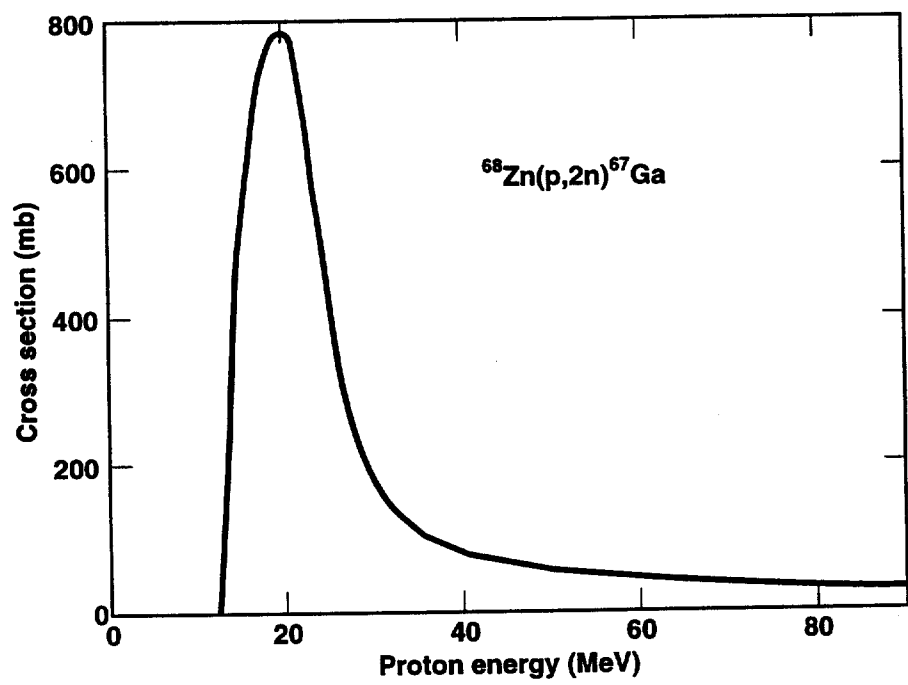


Figure 7b.

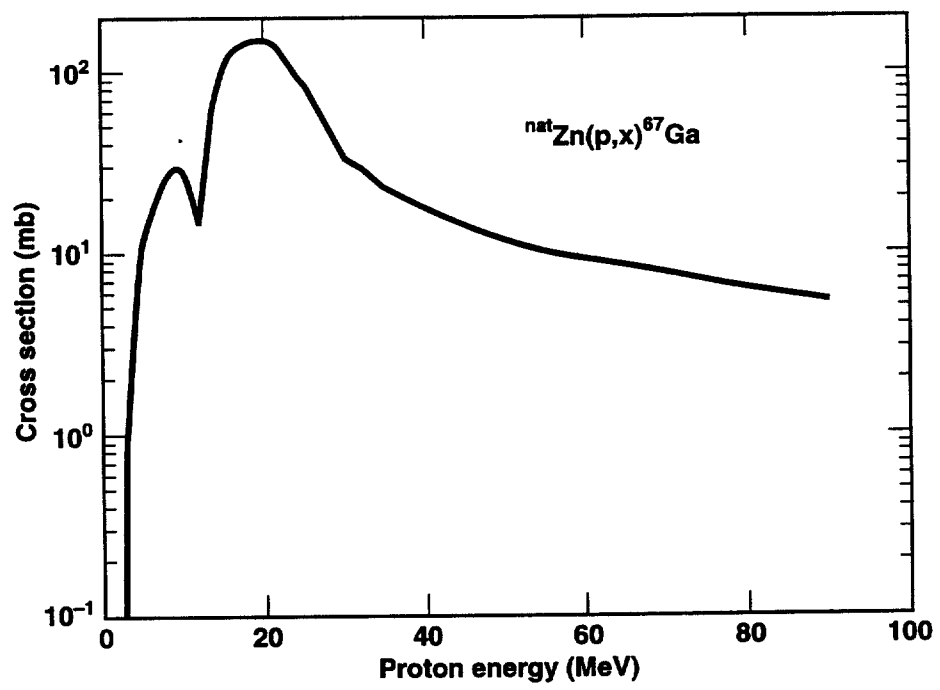


Figure 8a.

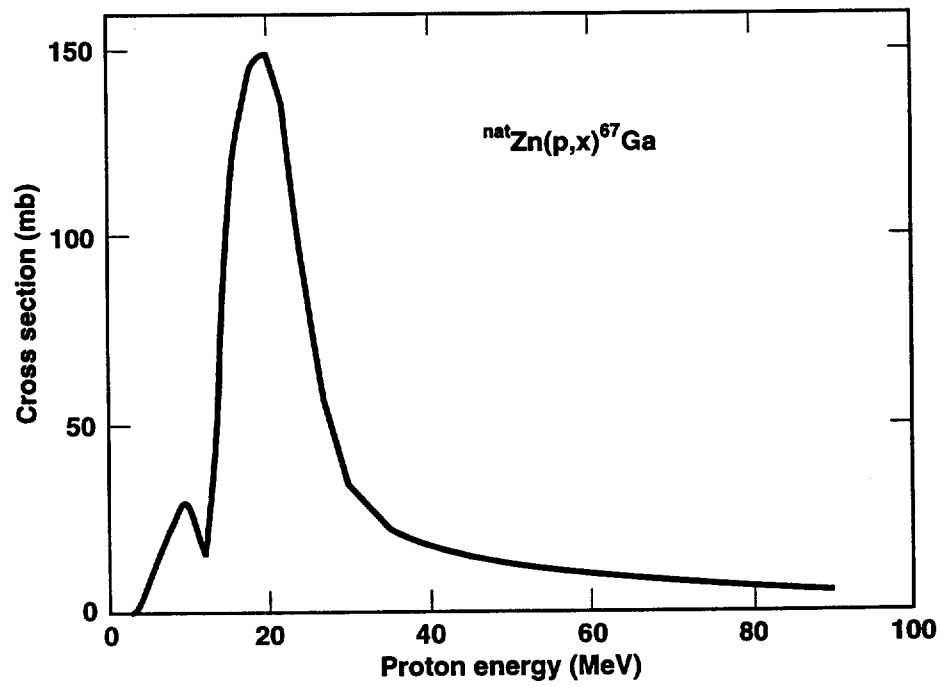


Figure 8b.

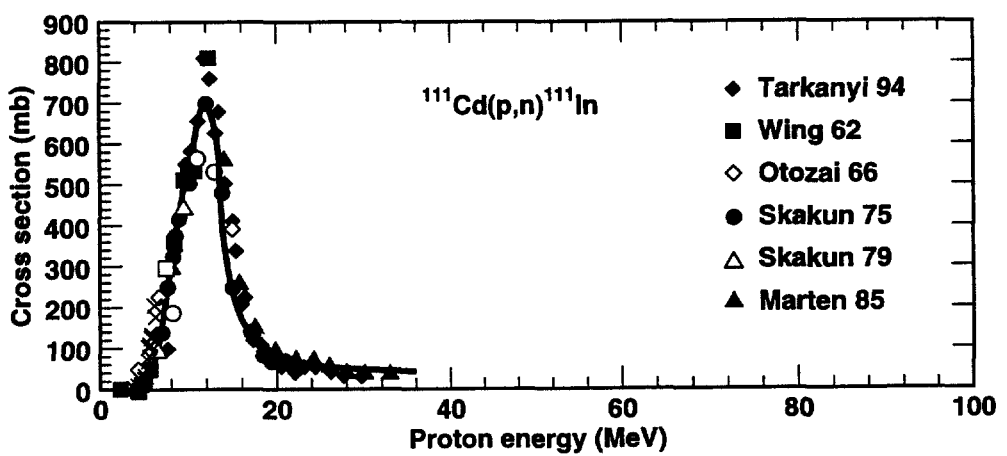


Figure 9.

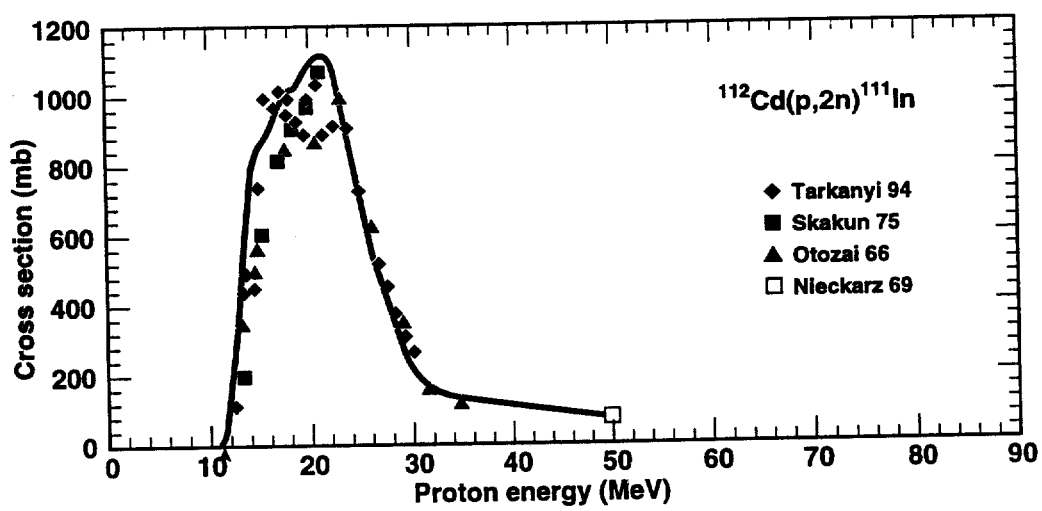


Figure 10.

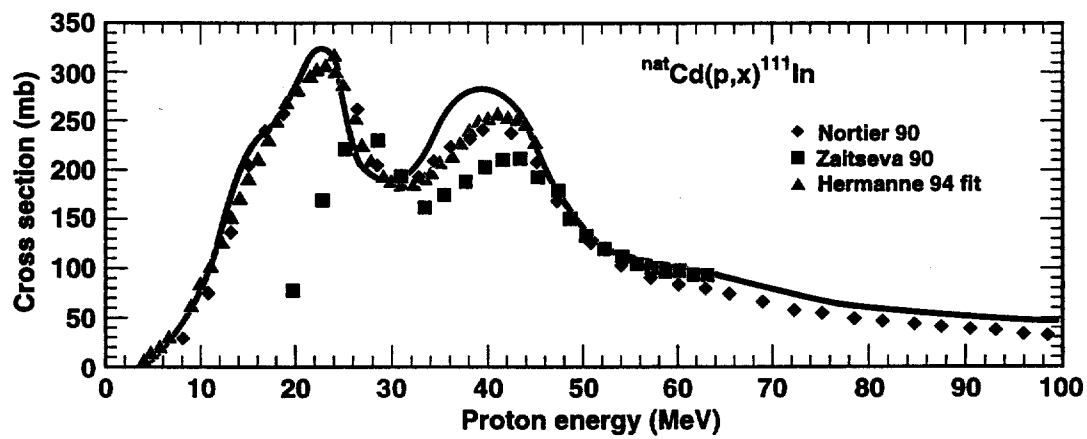


Figure 11a.

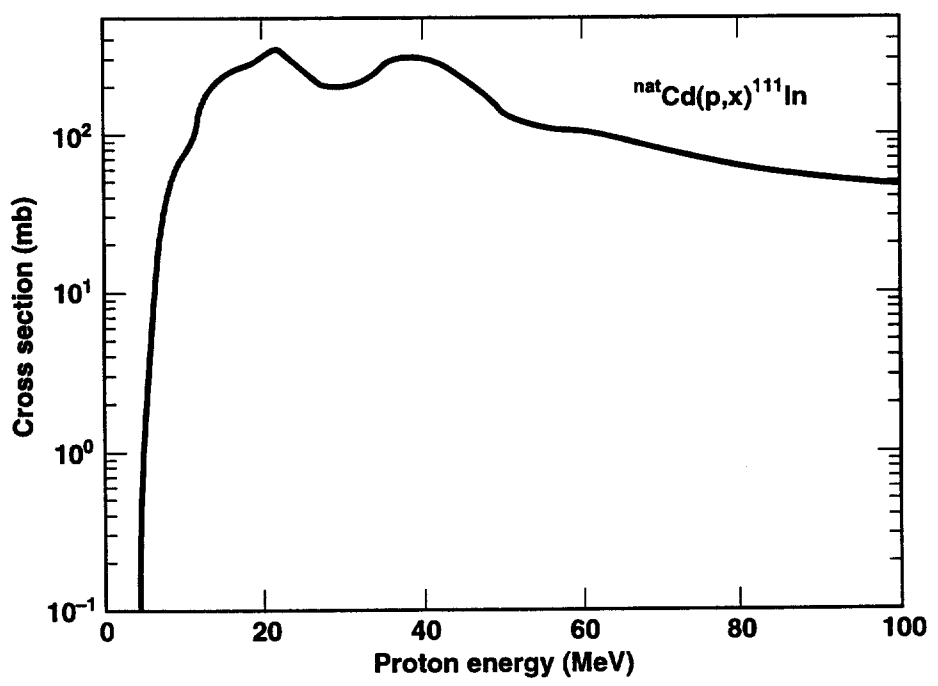


Figure 11b.

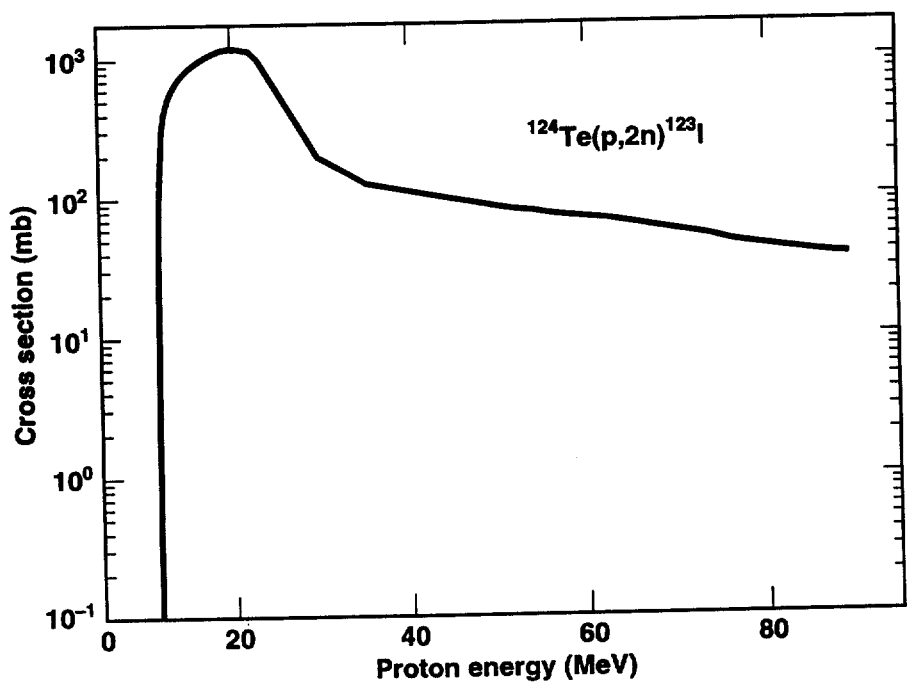


Figure 12a.

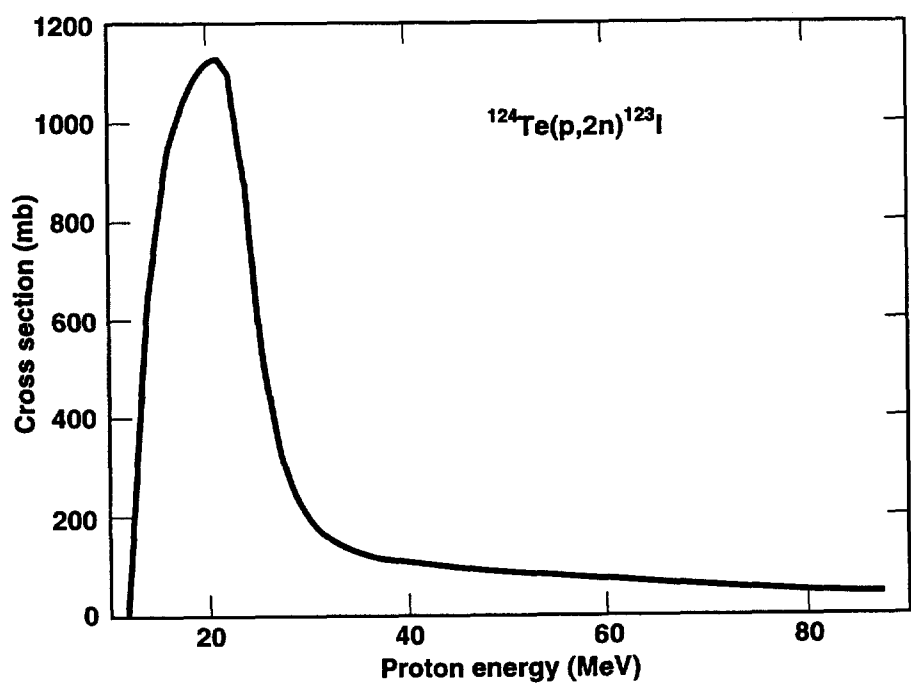


Figure 12b.

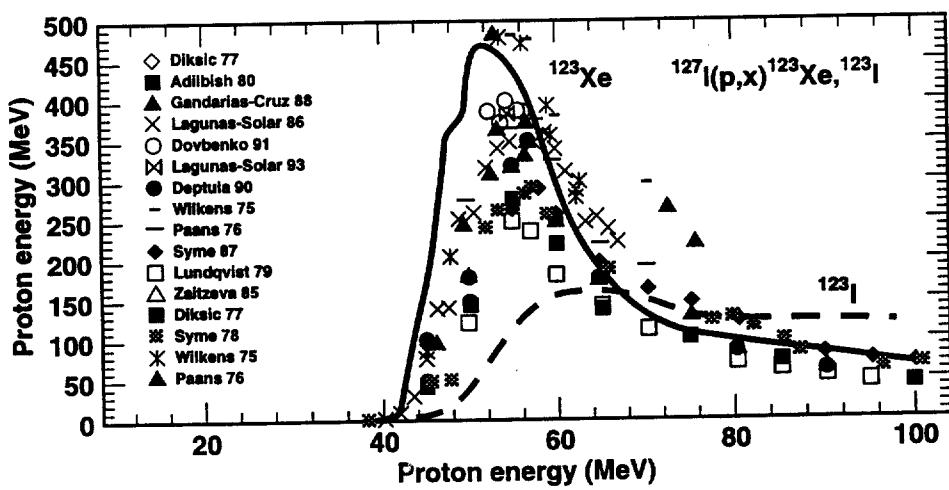


Figure 13a.

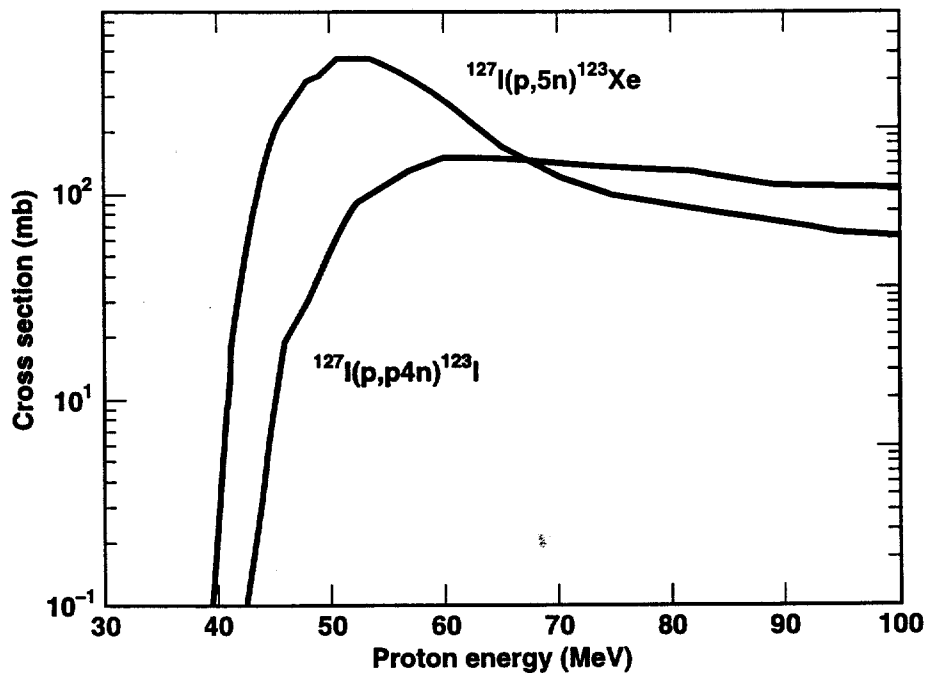


Figure 13b.

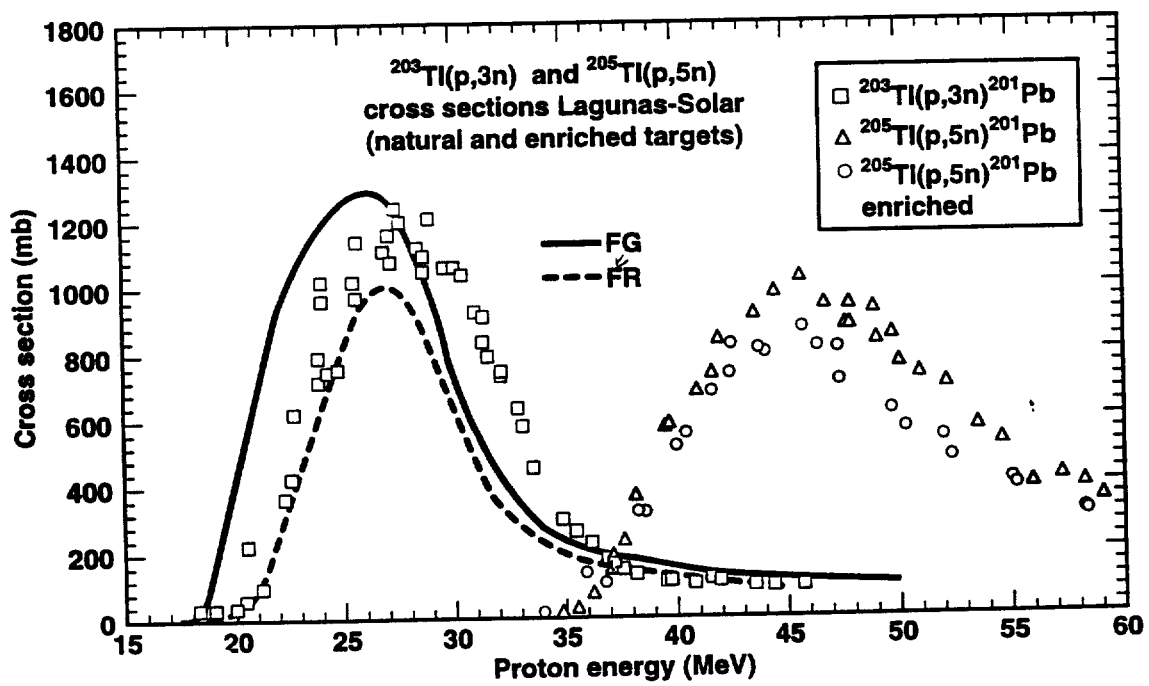


Figure 14a.

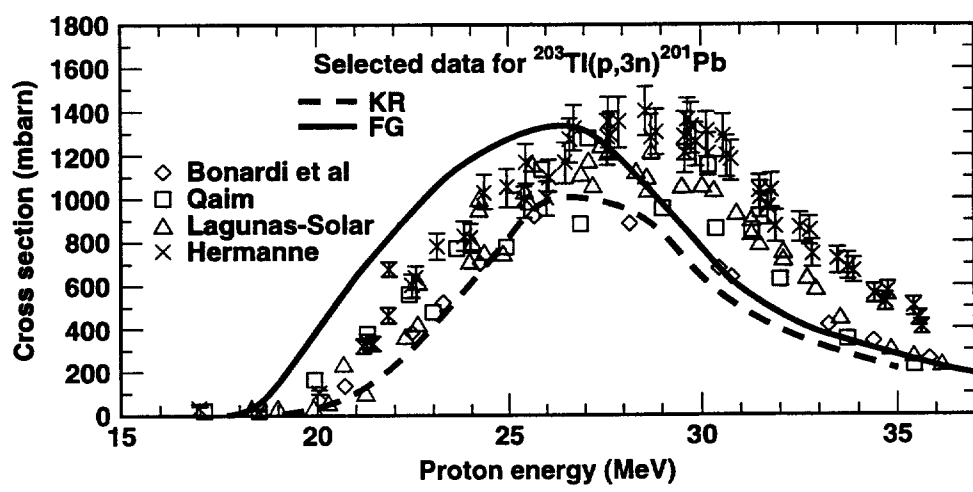


Figure 14b.

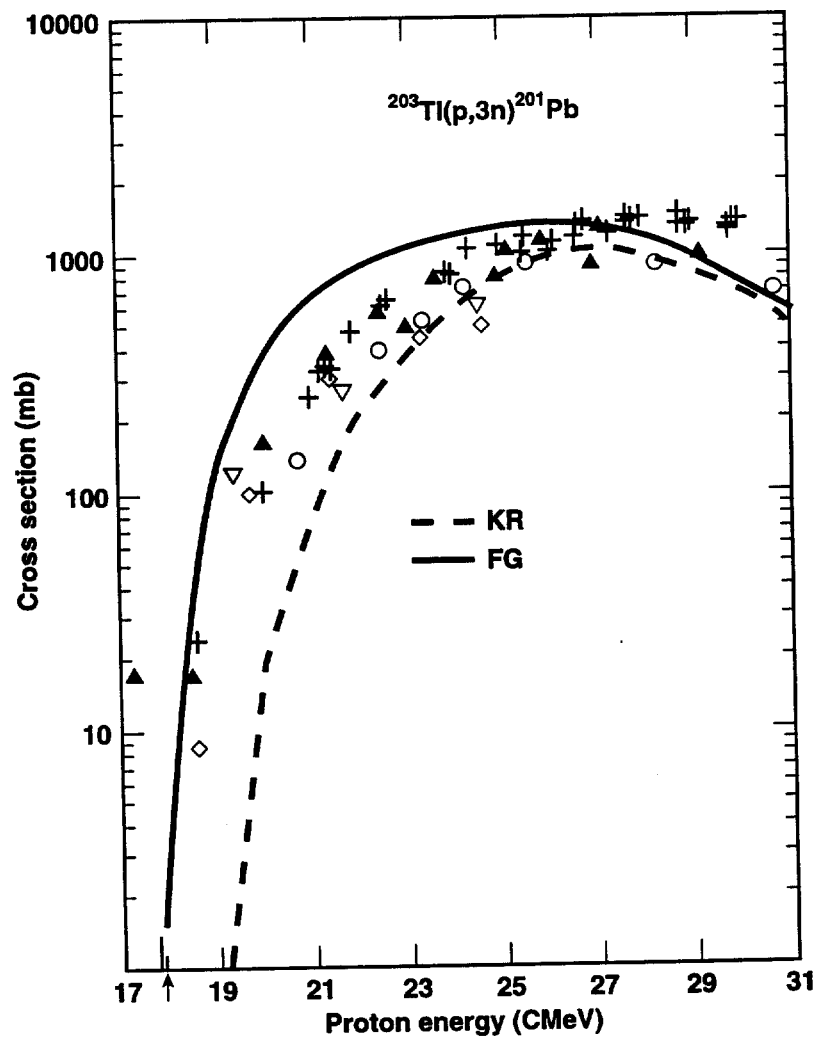


Figure 14c.